frontiers in Climate

ORIGINAL RESEARCH
published: 07 June 2021
doi: 10.3389/fclim.2021.688991

Compound Hot and Dry Events in Europe: Variability and Large-Scale Drivers

Monica Ionita[1]*, *Diana E. Caldarescu*[1] and *Viorica Nagavciuc*[1,2]

[1] Alfred Wegener Institute Helmholtz Center for Polar and Marine Research, Paleoclimate Dynamics Group, Bremerhaven, Germany, [2] Forest Biometrics Laboratory, Faculty of Forestry, Ştefan cel Mare University, Suceava, Romania

An important aspect of inevitable surprises, for the climate system, is the potential of occurrence of compound extreme events. These can be events that occur at the same time over the same geographic location or at multiple locations within a given country or around the world. In this study, we investigate the spatio-temporal variability of summer compound hot and dry (CHD) events at European level and we quantify the relationship between the occurrence of CHDs and the large-scale atmospheric circulation. Here we show that summer 1955 stands out as the year with the largest spatial extent characterized by hot and dry conditions (∼21.2% at European level), followed by 2015 (∼20.3%), 1959 (∼19.4%), and 1950 (∼16.9%). By employing an Empirical Orthogonal Function (EOF) analysis we show that there are three preferred centers of action of CHDs over Europe: Fennoscandia, the central part of Europe, and the south-eastern part of Europe. Overall, hot and dry summers are, in general, associated with persistent high-pressure systems over the regions affected by CHDs, which in turn reduces the zonal flow and diverts the storm tracks southward. The high-pressure systems associated with each mode of variability largely suppresses ascending motions, reduces water vapor condensation and precipitation formation, leading to drought conditions below this atmospheric system. This study may help improve our understanding of the spatio-temporal variability of hot and dry summers, at European level, as well as their driving mechanisms.

Keywords: drought, heatwave, compound events, atmospheric circulation, climate variability

OPEN ACCESS

Edited by:
Deepti Singh,
Washington State University Vancouver, United States

Reviewed by:
Ramiro I. Saurral,
University of Buenos Aires, Argentina
Kevin Grise,
University of Virginia, United States

***Correspondence:**
Monica Ionita
Monica.Ionita@awi.de

Specialty section:
This article was submitted to Predictions and Projections, a section of the journal Frontiers in Climate

Received: *31 March 2021*
Accepted: *14 May 2021*
Published: *07 June 2021*

Citation:
Ionita M, Caldarescu DE and Nagavciuc V (2021) Compound Hot and Dry Events in Europe: Variability and Large-Scale Drivers. Front. Clim. 3:688991. doi: 10.3389/fclim.2021.688991

INTRODUCTION

During the last decades a significant increase in the concurrence of hot summers and severe droughts has been observed (Seneviratne et al., 2012; Zscheischler et al., 2018; Feng et al., 2020; Raymond et al., 2020). The concurrence of dry and hot events is commonly known as "compound events" (Leonard et al., 2014). Compound events are events that occur at the same time or in sequence and at the same geographic location or at multiple locations within a country or around the world (Zscheischler et al., 2018; Raymond et al., 2020). Globally, an increase in the co-occurrence of hot and dry events over the observational period as well as in future projections has been found (Diffenbaugh et al., 2017; Zscheischler et al., 2018; Manning et al., 2019; Feng et al., 2020). The understanding of the spatio-temporal evolution and the large-scale drives of compound events is important because these events have often immediate impacts and can cause widespread

destruction in terms of societal and economical damages (Feng et al., 2020; Raymond et al., 2020). Overall, understanding the interactions between several number of competing events is much more complex than understanding the drivers of individual events.

Heatwaves and droughts are two of the most important natural hazards with significant impacts on the economy and society, around the world (Ciais et al., 2005; Kong et al., 2020). For example, severe heatwaves and droughts have struck Europe over the last decades (e.g., 2003, 2010, 2015, 2018) and caused significant human and monetary losses as well as environmental damages (Barriopedro et al., 2011; Ionita et al., 2017, 2020b; Ben-Ari et al., 2018). The financial losses due to the hot and dry conditions during summer 2018 alone were estimated to be ∼3.3 billion Euros, being the costliest single-event in Europe (Munich RE, 2020). In terms of compound hot and dry events at European level Manning et al. (2019), have shown that dry periods are becoming hotter, leading to an increase in the occurrence of long-lasting dry periods with extremely high temperatures and that the probability of such compound events (e.g., hot and dry) has increased across much of Europe over the last decades. Moreover, they have shown that the main driver of this change in the probability of occurrence of hot and dry events is due to the increasing temperatures throughout Europe. In their study centered over the Mediterranean region Russo et al. (2019), have shown that the hottest months are July and August, and are usually preceded by the occurrence of droughts in spring and early summer over the Iberian Peninsula, northern Italy, and the Balkans. In a recent study Bezak and Mikoš (2020), have shown that parts of Western Europe, Italy, the Balkan Peninsula, and Northern and Eastern Europe stand out as hotspots of compound drought and extreme heat events.

The co-occurrence of hot and dry events can be triggered by different mechanisms, like the land-atmosphere interactions and/or persistent large-scale atmospheric circulation patterns. The influence of the land-atmosphere interaction on the occurrence of compound hot and dry events has been found particularly significant during the warm season (Trenberth and Shea, 2005; Hirschi et al., 2011; Russo et al., 2019). One important factor which plays a significant role in the coupling between the land surface and the atmosphere is the soil moisture deficit (Hirschi et al., 2011; Seneviratne et al., 2012). Soil moisture deficit tends to reduce the evaporative cooling and to increase the sensible heat flux, thus leading to an increase in the surface temperature which in turn may result in heatwaves or it may exacerbate the prevailing drought conditions (Manning et al., 2018; Samaniego et al., 2018).

Compound events, like heatwaves and droughts, may also result as a consequence of persistent large-scale atmospheric circulation anomalies. One essential driver of heatwaves and droughts over Europe is the prevalence of long-lasting high-pressure systems, also known as atmospheric blocking (Barriopedro et al., 2011; Schubert et al., 2014, 2016; Ionita et al., 2017, 2020a). Atmospheric blocking is defined as a large-scale mid-latitude phenomenon, associated with persistent quasi-stationary high-pressure systems (Barriopedro et al., 2010). Overall, atmospheric blocking exerts significant impacts on different types of extremes such as heatwaves (Della-Marta et al., 2007; Barriopedro et al., 2011; Schubert et al., 2014), droughts (Schubert et al., 2016; Ionita et al., 2021), floods (Najibi et al., 2019; Ionita et al., 2020b), and cold spells (Hori et al., 2011; Rimbu et al., 2014). In general, dry and hot summers over Europe are associated with a high frequency of atmospheric blocking centered over the British Isle and/or over Fennoscandia (Della-Marta et al., 2007; Ionita et al., 2017; Bakke et al., 2020; Zhang et al., 2020).

So far, the analysis of compound hot and dry events (CHDs) over Europe has been focused either on particular regions (e.g., the Mediterranean region) or just by analyzing the trends of CHDs and their return values (Manning et al., 2019; Russo et al., 2019; Feng et al., 2020). In this study, we aim at making an in-depth analysis of the spatio-temporal variability of CHDs at European level as well as to quantify the relationship between the occurrence of CHDs and the large-scale atmospheric circulation. Improving our understanding of the physical processes behind the occurrence of compound hot and dry events could help for a better predictability and impact assessment of future CHDs, especially since the topic of predictability becomes essential in the view of an increase in the likelihood of extreme events in a warming climate. The outline of the study is as follows. The data and methods are described in section Data and Methods, while the main results and the discussion are shown in section Results and Discussion. The main conclusions of the paper are presented in section Conclusions.

DATA AND METHODS

In this study, drought conditions are defined by considering the 3-month Standardized Precipitation Index (SPI3) values <-1. For this analysis we used two SPI3 indices: the August SPI3 index based on all summer months (i.e., June-July-August), and the May SPI3 index which takes into account all spring months (i.e., March-April-May). The SPI index was extracted from the E-OBS v23.1e data set (https://surfobs.climate.copernicus.eu/dataaccess/access_eobs_indices.php), with a resolution of 0.1° x 0.1°. SPI takes into account the accumulated precipitation data, where the precipitation (PP) data has been fitted to a gamma distribution (McKee et al., 1993). Heatwave events are identified by employing a threshold-based methodology (Perkins and Alexander, 2013). This method considers periods of consecutive days with the daily maximum temperature (T_x) above a certain percentile of T_x for a particular calendar day. Here we employ the 90th percentile and a duration > 6 days (the 90th percentile is computed over the reference period 1971–2000). The heatwave duration index (HWDI) is defined as the number of days per season when the aforementioned criteria were fulfilled. The daily T_x data set has been extracted from the E-OBS v23.1e dataset (Cornes et al., 2018). The E-OBS data set builds on the European Climate Assessment and Dataset (ECA&D), which is a database of daily meteorological station observations across Europe. The station based data used to develop the gridded E-OBS data set are subjected to quality control and homogeneity test, thus, all series are checked for inhomogeneities. The E-OBS v23.1e dataset is

based on 100 realizations of each daily field (e.g., precipitation, daily mean temperature, daily maximum temperature, and daily minimum temperature). The spread of the E-OBS dataset is calculated as the difference between the 5th and 95th percentiles over the 100 realizations to provide a measure indicate of the 90% uncertainty range. For the current study we use the ensemble mean (the mean over the 100 realizations), which provides a "best guess" value. In order to isolate T_x values from the global warming sign, before the computation of HWDI, we removed the linear trend from the entire daily T_x dataset, by applying a 1st degree polynomial regression technique. A similar approach has been used recently by Geirinhas et al. (2021) in order to remove the global warming signal from the maximum temperature to compute heatwave events in southeast Brazil. Considering our definition of drought and daily heatwave episodes, a compound hot and dry event (CHD) is then defined as a combined index when a heatwave episode occurs during a period under drought conditions (i.e., a summer with an associated 3 month SPI value (SPI3 August) <-1). This metric has been successfully applied also for other regions (Russo et al., 2019; Geirinhas et al., 2021). For our analysis we used only the grid points which are satisfying the compound event criteria. The analysis was made for the whole summer (June-July-August) season.

To understand the role of large-scale atmospheric circulation in determining the spatio-temporal variability of CHD events, we used the monthly geopotential height, the zonal and meridional wind at 500 mb (Z500). The datasets were extracted from the ERA5 reanalysis project (Hersbach et al., 2020), which has a spatial resolution of $0.25^\circ \times 0.25^\circ$ and covers the period 1950–2020.

The patterns of the dominant modes of CHD variability are based on Empirical Orthogonal Function (EOF) analysis (von Storch and Zwiers, 1999). The EOF technique aims at finding patterns in an existing data set that explains the most variance through a linear combination of the original variables, and it represents an efficient method of investigating the spatial and temporal variability of time series which cover large areas. The EOFs resulting from the standardized and detrended CHD data set (anomaly divided by standard deviation) allow us to recognize the regions with different climatology and filter out some errors in the data.

RESULTS AND DISCUSSION

Historical Evolution of Compound Events (Hot and Dry)

The association between the occurrence of hot extreme temperatures and the surface moisture deficit, as captured by the SPI index, has been tested both with lag (SPI leads HWDI) and in-phase. When performing the lag analysis, significant correlations are found over the central part of the Iberian Peninsula, France, Italy, and the central part of Ukraine (**Figure 1A**). The lag correlation indicates that over the aforementioned regions the spring drought conditions could be used as an indicator for the upcoming summer heatwaves. This lagged relationship is in agreement with previous studies, which have shown that drought conditions in spring and the beginning of summer have the tendency to amplify hot extremes especially over the southern part of Europe, via the land-atmosphere feedbacks (Fischer et al., 2007; Mueller and Seneviratne, 2012).

The in-phase correlation map (**Figure 1B**) indicates that summer heatwaves over large areas in Europe co-occur with dry summers. The highest correlations are found over the British Isles, Germany, the north-eastern part of France, and the south-eastern part of Europe. Over these regions the correlation is significant (99% significance level) and the highest amplitude (up to 0.8) is observed over the south-eastern Europe and the British Isles. An interesting feature of the correlation maps between SPI3 and the HWDI is the fact that over the Iberian Peninsula and the southern France the correlations are significant when SPI3 leads HWDI (SPI3 May vs. HWDI JJA), while for the rest of Europe the highest significant correlations are found in-phase (SPI3 August vs. HWDI JJA). The lag-relationship over the Iberian Peninsula has been also found by Russo et al. (2019). In their study, Russo et al. (2019) have shown that extreme high temperatures in summer over the Iberian Peninsula and northern Italy are preceded by the extremely dry condition in spring.

Figure 1 shows a clear signal that hot summers tend to co-exist with dry summers. To test the spatial distribution and the variability of compound hot and dry events, in summer, we have analyzed the frequency of CHD over the 1951–2020 period (**Figure 2**). Since our aim is to test if there are changes in the frequency of CHD events on decadal time scales, we have splitted our data into shorter time periods (e.g., 10 years) and computed the number of CHDs/decades. Over the decade 1951–1960, CHD events were recorded over the south-eastern Europe, Fennoscandia, and western Russia (**Figure 2A**). The highest number of CHDs/decade (up to three events) was recorded over the southwestern part of Romania and the western part of Russia. The decades 1961–1970 (**Figure 2B**) and 1981–1990 (**Figure 2D**) indicate an overall lack of CHDs, with small exceptions (1 CHD/decade) over small regions in central Europe and Fennoscandia. The decade 1971–1980 (**Figure 2C**) indicates the occurrence of 1-2 CHD events/decade over the northern part of Europe and Fennoscandia and no CHD's over the southern part of Europe. Over the decade 1991–2000, CHD events were more frequent (1-2 CHD/decade) mainly over the eastern part of Europe (**Figure 2E**). Throughout the decade 2001–2010 (**Figure 2F**) at least 1 CHD/decade was recorded over large areas in Europe, while over small regions in Spain, southern France, and southern Russia, 2-3 CHDs/decade have been recorded. The regions where the CHD are recorded during this decade, are the regions where the 2003 and 2010 heatwaves had the highest amplitude (Schär et al., 2004; Barriopedro et al., 2011). Compared with the previous decades, the period 2011–2020 (**Figure 2G**) is characterized by an increase in the number of CHD events/decade ($\sim$4 CHD/decade), especially over the central and south-eastern part of Europe. The increase in the number of CHD events over the south-eastern part of Europe is mainly due to an increase both in the duration of heatwaves over this region (**Figure 3A**) as well as in the frequency of the HW events

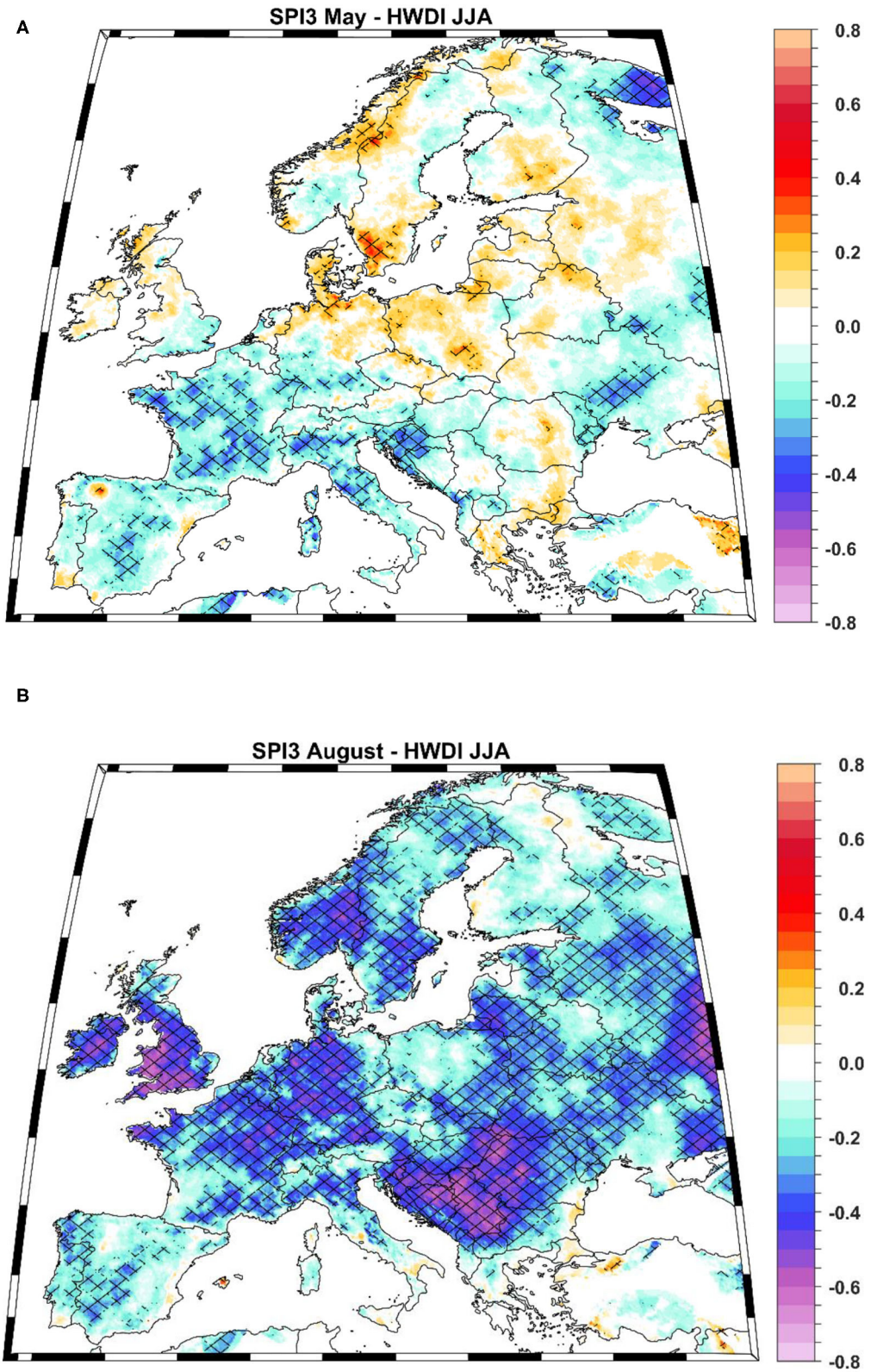

FIGURE 1 | (A) Correlation map between May SPI3 and HWDI over the period 1950–2020 and **(B)** as in **(A)** but for August SPI3. Hatching indicates the grid points where the correlations are significant (99% significance level).

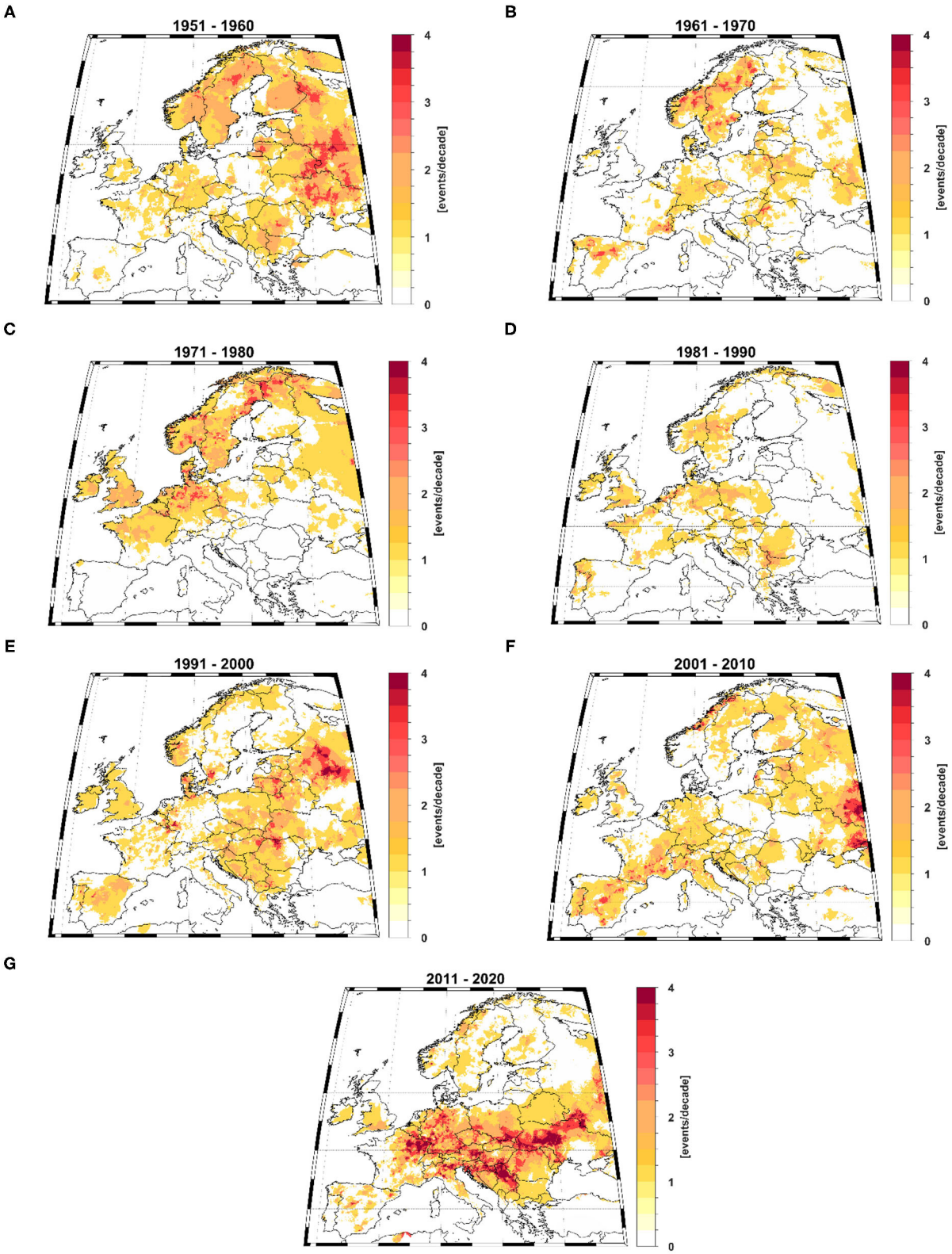

FIGURE 2 | Decadal frequency of compound hot and dry events (CHD) over the period 1951–2020. **(A)** 1951–1960; **(B)** 1961–1970; **(C)** 1971–1980; **(D)** 1981–1990; **(E)** 1991–2000; **(F)** 2001–2010; and **(G)** 2011–2020.

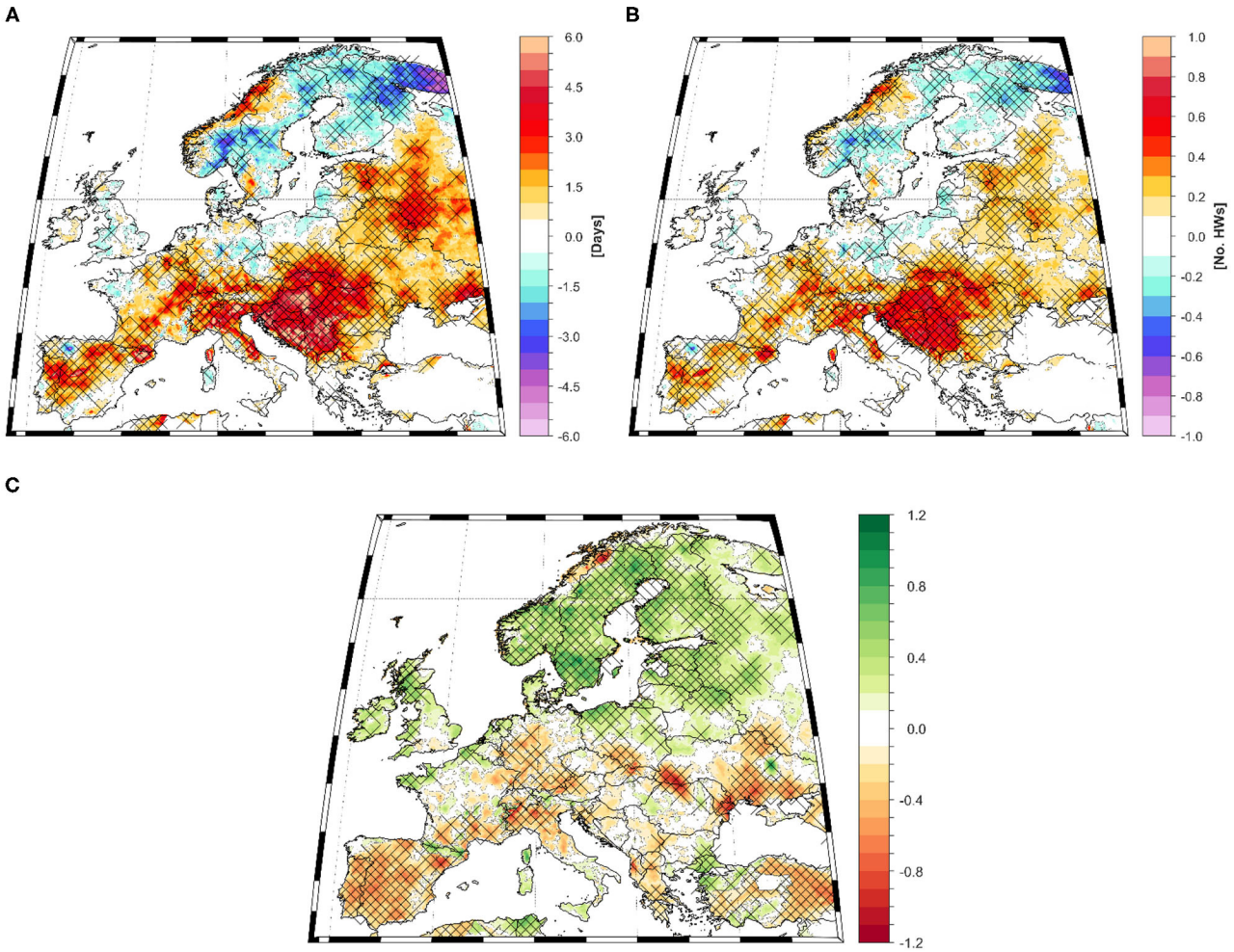

FIGURE 3 | Changes over the period 1986–2020 relative to 1950–1985 for **(A)** the heat wave duration index (HWDI) for summer (June-July-August); **(B)** as in **(A)** but for the heatwaves frequency and **(C)** as in **(A)** but for August SPI3. The hatched areas indicate significant changes at 99% significance level based on a *Student t-test*.

(**Figure 3B**). Overall, August SPI3 indicates an overall wetting over the northern part of Europe and a drying tendency over the southern part of Europe (**Figure 3C**), which is in agreement with previous studies regarding the change in the occurrence of drought events over Europe, based on the SPI drought index (Ionita and Nagavciuc, 2021; Vicente-Serrano et al., 2021).

The increase in the number of CHD events over the last two decades (**Figures 2F,G**) is also visible in terms of the spatial extent of these CHDs. Over the analyzed period, there is a strong variability in the percent of the area covered by CHDs (**Figure 4**). Summer 1955 stands out as the year with the largest spatial extent under both hot and dry conditions at European level (∼21.2%), followed by 2015 (∼20.3%), 1959 (∼19.5%), and 1950 (∼16.9%). A detailed description of some of these extreme events will be given in section Spatio-Temporal Variability of Hot and Dry Summers and **Supplementary Table 1**.

Spatio-Temporal Variability of Hot and Dry Summers

The patterns of the dominant modes of CHD variability are based on the Empirical Orthogonal Function (EOF) analysis (von Storch and Zwiers, 1999). In this study, we consider only the first three EOFs patterns which explain ∼28% of the total variance. The leading EOF (EOF1, **Figure 5A**) accounts for 10.9% of the total variance, the second EOF (EOF2, **Figure 8A**) accounts for 9.7% of the total variance and the third EOF (EOF3, **Figure 11A**) explains 7.4% of the total variance. These EOF's are well-separated according to the North rule (North et al., 1982).

First Mode of Variability and Large-Scale Drivers

The first EOF (**Figure 5A**) has a dipole-like structure, with the highest positive loadings over Fennoscandia and western Russia and negative loadings over Romania, Hungary, and western Bulgaria. This dipole-like structure emphasizes that the CHD variability over Fennoscandia and the western part of Russia is

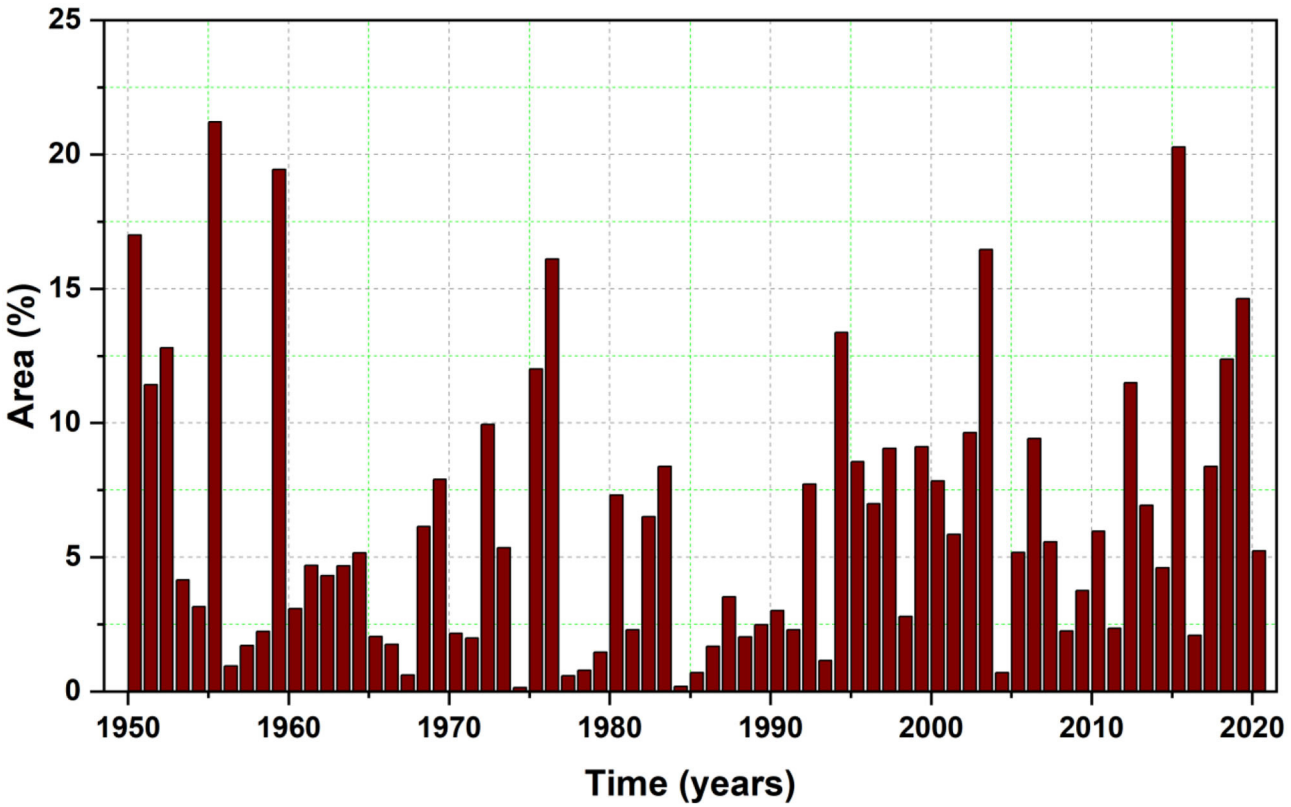

FIGURE 4 | Temporal evolution of the percentage area (11°E–40°E, 35°N–72°N) affected by compound hot and dry events over the period 1950–2020.

influenced by the same factors (e.g., the large-scale circulation). The driest and warmest summers over Fennoscandian and western Russia, in terms of summer PC1 (**Figure 5B**), were recorded for the years 1955, 1959, 1975, 1997, and 2006. The amplitude of the loadings over the southern part of Europe are much smaller compared to the positive ones over Fennoscandia, thus we argue that EOF1 is a good indicator for the spatio-temporal variability of CHD over the northern part of Europe.

The composite map of Z500 anomalies and the corresponding wind vectors for hot and dry years over Fennoscandia and the western part of Russia, as identified by PC1 (**Figure 5B**), is characterized by a tripole-like structure, with negative Z500 anomalies over Greenland, positive Z500 anomalies extending from the eastern coast of U.S. to the northern part of Europe and negative Z500 anomalies centered over the Mediterranean region (**Figure 5C**). This pattern resembles the Scandinavian blocking pattern (van der Wiel et al., 2019). The high-pressure system centered over Fennoscandia reduces the zonal flow and diverts the storm tracks southward, and the regions situated under the influence of this system experience warmer and drier than normal conditions due to the advection of warm and dry air from the eastern part of Europe and enhanced incoming solar radiation (Bueh and Nakamura, 2007).

Two of the most extreme hot and dry events, over Fennoscandia and the western part of Russia, as captured by the amplitude of the PC1 time series (**Figure 5B**) were recorded in summer 1955 and summer 1959, respectively. The summer 1955 and 1959 heatwave and drought as measured by the rank maps of the summer HWDI, summer T_x and August SPI3 are shown in **Figure 6**. The most-affected regions during the summer 1955 event were the southern part of Fennoscandia, in terms of heatwave duration (**Figure 6A**), small parts of Norway in terms of extreme temperatures (**Figure 6C**), and the whole Fennoscandia and western part of Russia, in terms of drought amplitude (**Figure 6E**). Summer 1955 ranks as the longest one in terms of heatwave duration, over the study period (i.e., 1950–2020), over the southern part of Norway and Sweden, and as the driest one over large regions covering Norway, Finland, Sweden, and western Russia (**Figure 6E**). In summer 1955 there were more than 20 days/season characterized by heatwaves (**Figure 7A**) and the August SPI3 index reached values up to −3 over large parts in the northern part of Europe (**Figure 7C**). This particular summer was characterized by extreme large-scale circulation anomalies (**Figure 7E**) which resemble the pattern associated with high values of PC1 (**Figure 5C**). Summer 1955 was characterized by negative Z500 anomalies over Greenland, positive Z500 anomalies over Fennoscandia, and negative z500 anomalies centered over the Mediterranean region. The 1959 event was more restricted, in terms of spatial extent, compared to the 1955 event (**Figures 6B,D,F**). Summer 1959 ranks as the

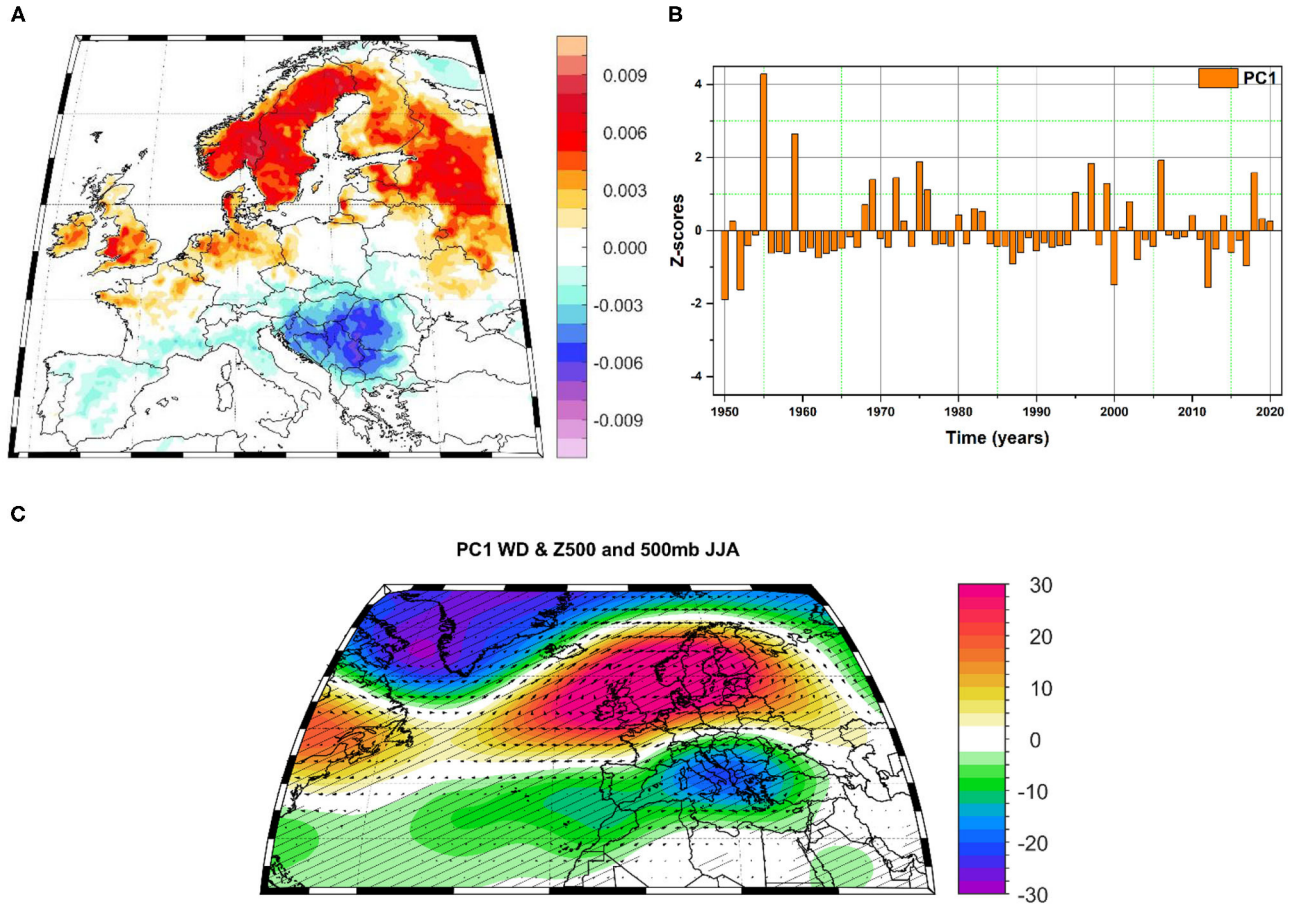

FIGURE 5 | Spatio-temporal variability of compound hot and dry events over the period 1950–2020. **(A)** First spatial pattern (EOF1); **(B)** the temporal evolution (PC1) corresponding to EOF1; **(C)** The high (PC1 > 1 standard deviation) composite map between PC1 and the summer (JJA) Z500 and the wind vectors at 500 mb. Units: **(C)** Z500 [m].

longest one in terms of heatwave duration (**Figure 6B**) over small areas in the north-western part of Russia, and as the driest one in the southern part of Sweden and small regions in western Russia (**Figure 6D**). In summer 1959, there were up to 20 days/season characterized by heatwaves (**Figure 7B**). The magnitude of the 1959 drought event was smaller (in terms of amplitude) compared to the 1955 event (**Figure 7D**). The prevailing large-scale atmospheric circulation associated with the 1959 events resembles the one in summer 1955, with positive Z500 anomalies over Fennoscandia flanked by negative Z500 anomalies over Greenland and the Mediterranean Sea (**Figure 7F**).

Second Mode of Variability and Large-Scale Drivers

The second EOF pattern (**Figure 8A**) describes 9.7% of the total variance of the summer CHD variability and is characterized by positive loadings over central Europe, with the highest amplitude over Germany. Summer PC2 (**Figure 8B**) is characterized by interannual variability with driest and warmest summers, in terms of summer PC2 amplitude, recorded for the years 1976, 2003, 2015, 2018, and 2019. The spatio-temporal structure of EOF2 captures best the extremely warm and dry summer over the last two decades (e.g., 2003, 2015, and 2018) (Schär et al., 2004; Ionita et al., 2017, 2020a; Bakke et al., 2020; Ionita and Nagavciuc, 2020).

The composite map of Z500 anomalies and the corresponding wind vectors for hot and dry years over central Europe, as identified by PC2 (**Figure 8B**), is characterized by a wave train with positive Z500 anomalies over the eastern coast of the U.S., negative Z500 anomalies over central North Atlantic Ocean, positive Z500 anomalies over central Europe and negative Z500 anomalies over western Russia (**Figure 8C**). The wave-train like pattern of alternating Z500 anomalies, resembling an Ω-like blocking pattern, suggests a stationary Rossby wave signal which is usually associated with droughts and heatwaves over the Eurasian continent (Ionita et al., 2012, 2015; Schubert et al., 2014).

Two of the most extreme hot and dry events, over the central part of Europe, as captured by the amplitude of the PC2 time series (**Figure 8B**) were recorded in summer 2003

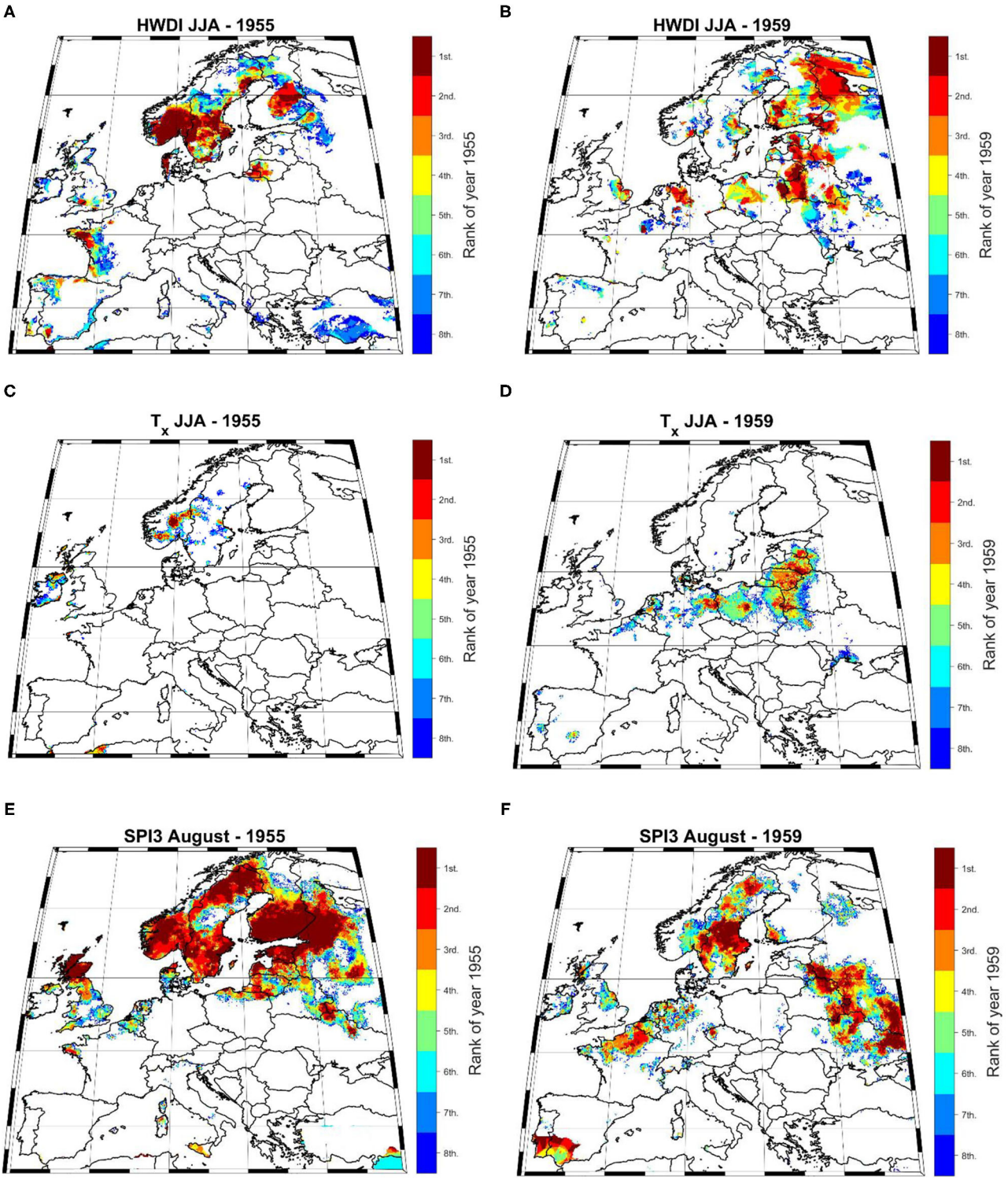

FIGURE 6 | (A) Top-eight ranking of summer 1955 HWDI; **(B)** Top-eight ranking of summer 1959 HWDI; **(C)** Top-eight ranking of summer 1955 T_x; **(D)** Top-eight ranking of summer 1959 T_x; **(E)** Top-eight ranking of 1955 August SPI3; **(F)** Top-eight ranking of 1959 August SPI3; 1st means the longest heatwave (HWDI), hottest (T_x), and driest (SPI3) since 1950, 2nd signifies the second longest, hottest and/or driest, etc., and all ranks >8 are shown in white. Analyzed period: 1950–2020.

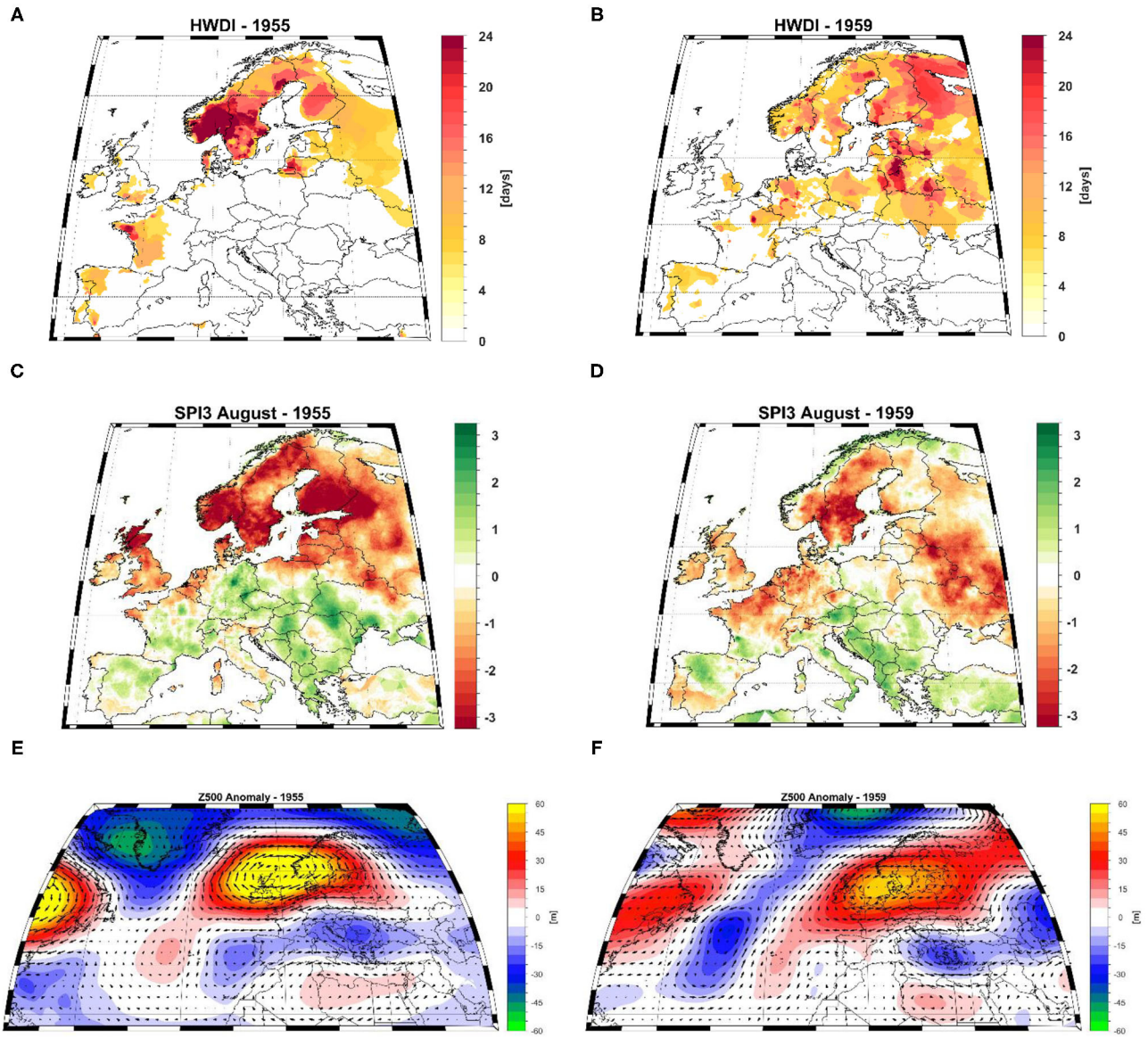

FIGURE 7 | Study cases 1955 and 1959. **(A)** HWDI−1955, **(B)** HWDI−1959; **(C)** August SPI3–1955; **(D)** August SPI3–1959; **(E)** Summer Z500 anomalies−1955 and **(F)** Summer Z500 anomalies−1959. The anomalies are computed relative to the period 1971–2000.

and summer 2015, respectively. Summer 2003 experienced the longest heatwave (**Figure 9A**) and the warmest summer on record over most of central Europe, including the northwestern parts of Spain, France, Italy, Germany, Switzerland, and Austria, and the western part of the Czech Republic (**Figure 9C**). In terms of drought, summer 2003 was among the driest one over small areas in the southern part of Germany and northern part of Italy (**Figure 9E**). The 2003 event was much clearly visible in terms of heat wave duration, and to a lesser extent in terms of drought. In summer 2003 there were more than 40 days/season characterized by extremely high temperatures (**Figure 10A**) and the August SPI3 index reached values up to −3 over large parts of the central part of Europe (**Figure 10C**). This particular summer was characterized by extreme large-scale circulation anomalies (**Figure 10E**) which resemble a Rossby wave train, similar to the one associated with high values of PC2 (**Figure 8B**). Summer 2003 was characterized by negative Z500 anomalies over the central North Atlantic Ocean, positive Z500 anomalies over central Europe, and negative Z500 anomalies over western Russia.

The 2015 event, was shifted toward the eastern part of Europe compared to the 2003 event. In 2015, the longest heatwave (**Figure 9B**) and the hottest regions were the southern part of Germany, the Czech Republic, eastern part of Austria, and

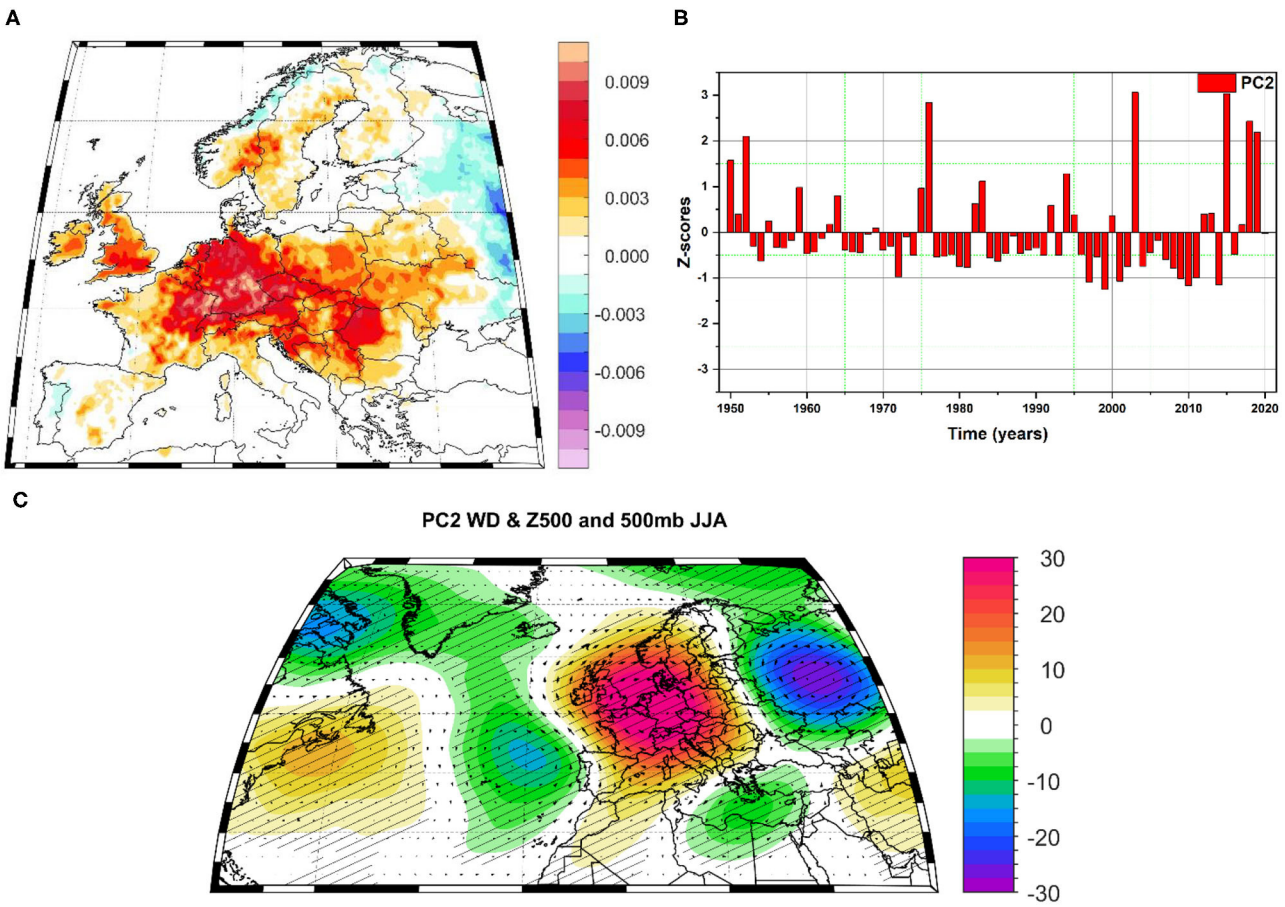

FIGURE 8 | Spatio-temporal variability of compound hot and dry events over the period 1950–2020. **(A)** Second spatial pattern (EOF2); **(B)** the temporal evolution (PC2) corresponding to EOF2; **(C)** The high (PC2 > 1 standard deviation) composite map between PC2 and the summer (JJA) Z500 and the wind vectors at 500 mb. Units: **(C)** Z500 [m].

small regions from the eastern part of Europe (**Figure 9D**). Summer 2015 was also the driest one on record over the eastern part of Austria, the eastern part of Poland, the western part of Ukraine, and eastern part of Belarus (**Figure 9F**). In summer 2015 there were up to 25 days/season characterized by extremely high temperatures (**Figure 10B**) and the August SPI3 index reached the highest amplitude over the central and eastern part of Europe (**Figure 10D**). In summer 2015, the Z500 anomalies are projecting onto an Ω-like block pattern with negative Z500 anomalies over the middle of the North Atlantic Ocean, an anomalous positive center of Z500 anomalies over central Europe, and negative z500 anomalies over western Russia (**Figure 10F**). Under the influence of Ω blocks and northward shifted storm tracks, warm dry air from southern Europe and Africa was pulled northward, pushing temperatures higher than normal over the Iberian Peninsula, central Europe, and the Balkans.

Third Mode of Variability and Large-Scale Drivers

The third EOF pattern (**Figure 11A**) describes 7.4% of the total variance of the summer CHD variability and is characterized by positive loadings over south-eastern Europe (i.e., Romania, Bulgaria, Hungary, Serbia, Croatia), negative but very weak (in terms of amplitude) loadings over Poland and Ukraine and positive, but weak, amplitudes over the northern part of Finland. The driest and warmest summers, based on the temporal evolution of summer PC3 (**Figure 11B**), were recorded for the years 1950, 1955, 1980, 1998, 2000, 2003, 2006, and 2012.

The composite map of Z500 anomalies and the corresponding wind vectors for hot and dry years over the south-eastern part of Europe, as identified by PC3 (**Figure 11C**), is characterized by a wave train with negative Z500 anomalies over the central North Atlantic Ocean, positive Z500 anomalies over the south-eastern part of Europe coupled to another center of positive Z500 anomalies over Fennoscandia and negative Z500 anomalies over western Russia (**Figure 11C**). This kind of pattern favors the advection of dry and warm air from the southeastern part of Europe, reduced precipitation, and high temperatures over the region situated under the influence of the high-pressure system. For the case studies, based on the PC3 amplitude, we have chosen the years with the highest amplitude: 1950 and 2012, respectively.

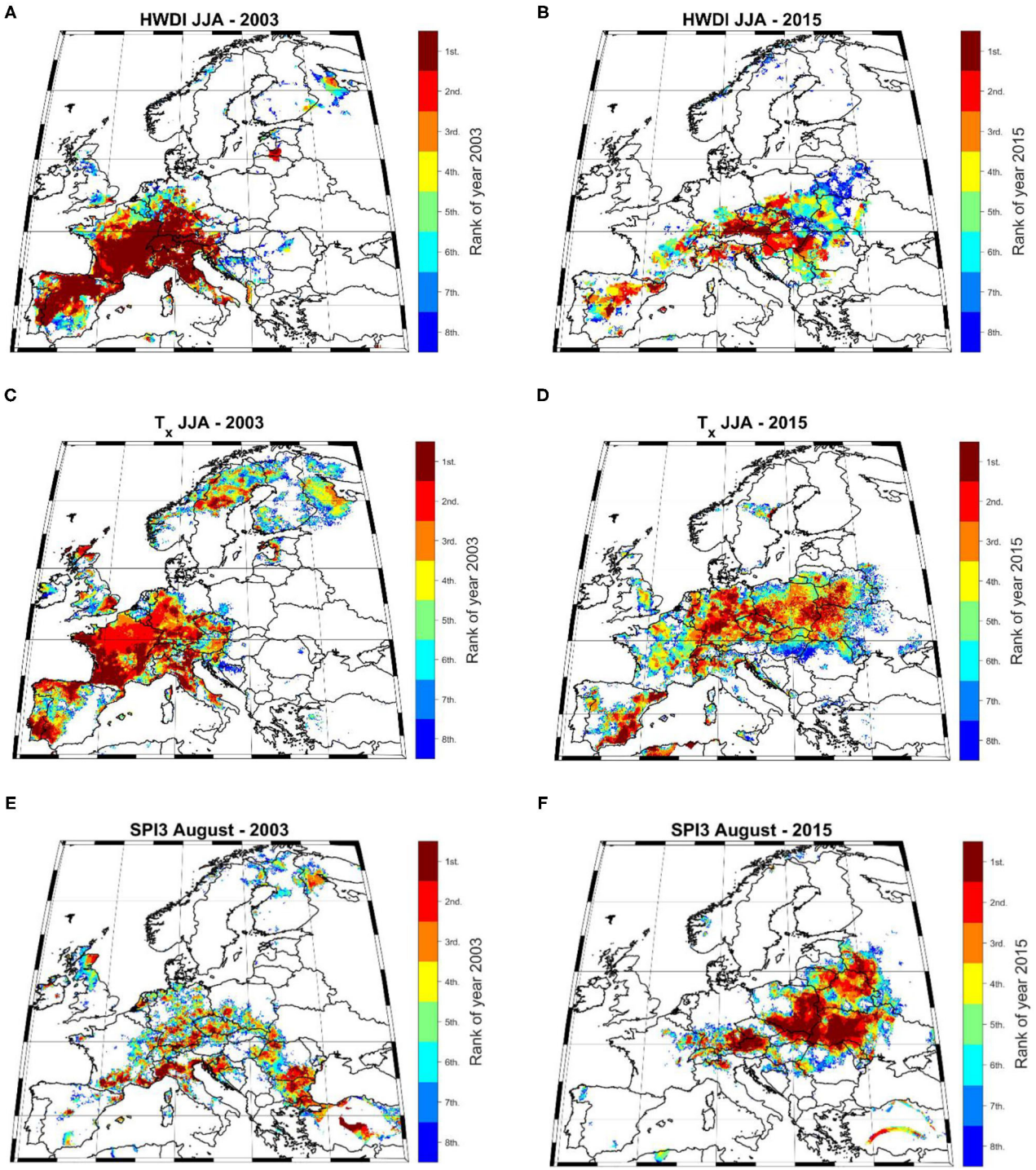

FIGURE 9 | (A) Top-eight ranking of summer 2003 HWDI; **(B)** Top-eight ranking of summer 2015 HWDI; **(C)** Top-eight ranking of summer 2003 T_x; **(D)** Top-eight ranking of summer 2015 T_x; **(E)** Top-eight ranking of 2003 August SPI3; **(F)** Top-eight ranking of 2015 August SPI3. 1st means the longest heatwave (HWDI), hottest (T_x), and driest (SPI3) since 1950, 2nd signifies the second longest, hottest and/or driest, etc., and all ranks >8 are shown in white. Analyzed period: 1950–2020.

In summer 1950 record breaking heatwaves were observed over small regions in the southern part of Europe (**Figure 12A**) and record-breaking temperatures were observed in the southern part of Hungary and Croatia (**Figure 12C**), but this summer was the driest one on record over the northern part of Finland and small regions over the southern part of Europe (i.e., Croatia, Bosnia

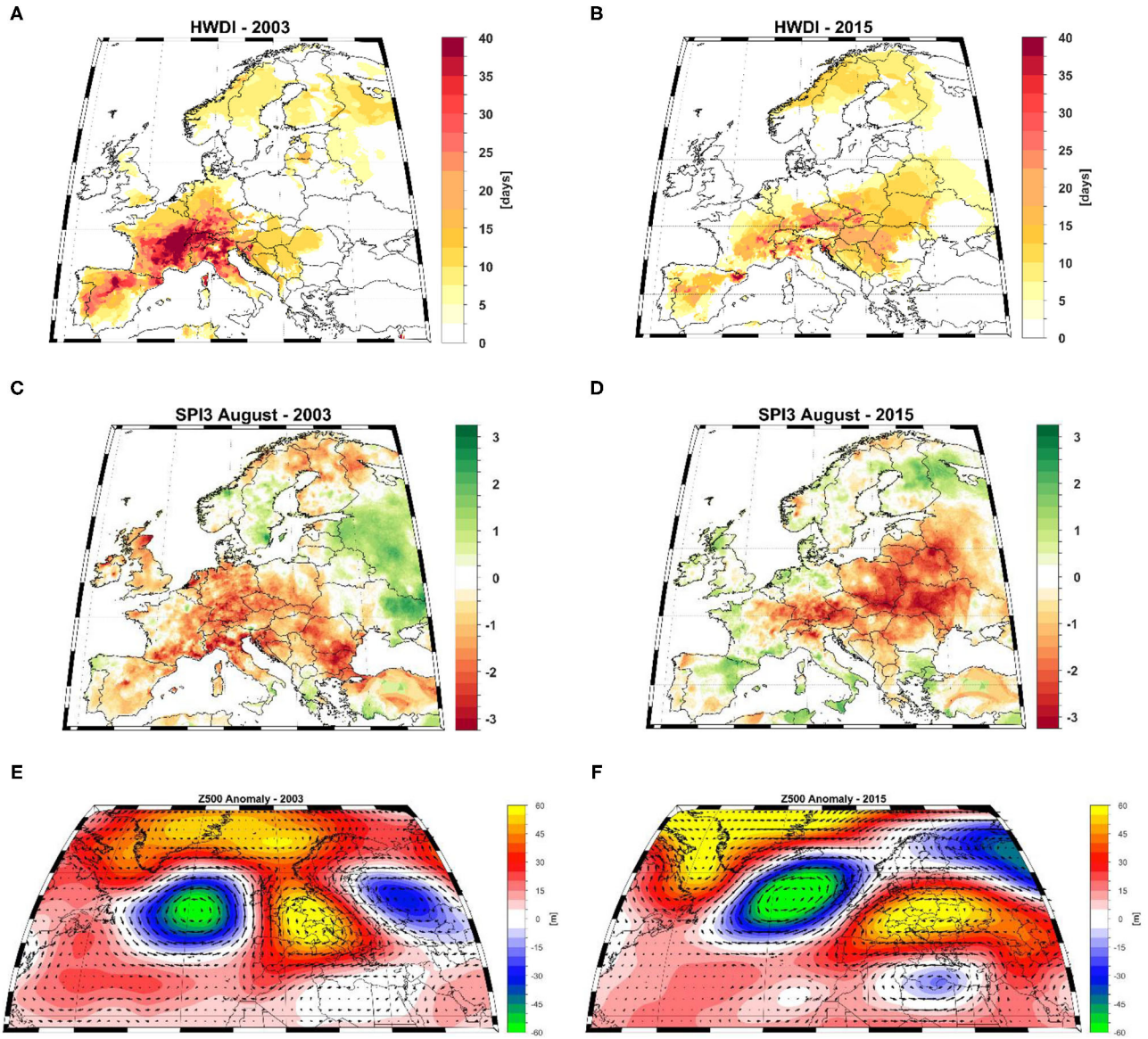

FIGURE 10 | Study cases 2003 and 2015. **(A)** HWDI−2003, **(B)** HWDI−2015; **(C)** August SPI3–2003; **(D)** August SPI3–2015; **(E)** Summer Z500 anomalies−2003 and **(F)** Summer Z500 anomalies−2015. The anomalies are computed relative to the period 1971–2000.

and Herzegovina, Romania) (**Figure 12E**). In summer 1950 there were up to 18 days/season of extremely high temperatures (**Figure 13A**) over the southern part of Europe, with a focus on Croatia, Bosnia, and Herzegovina, Serbia, and the western part of Romania, complemented by extremely dry conditions over these regions (**Figure 13C**). Dry conditions were recorded also over Finland and the north-western part of Russia, but over this region no heatwaves were recorded (**Figure 13A**). The large-scale atmospheric circulation, throughout summer 1950 was characterized by a wave train-like in the Z500, with negative Z500 anomalies over the central North Atlantic Ocean, positive Z500 anomalies over southern Europe and the Mediterranean Sea, and negative Z500 anomalies over western Russia (**Figure 13E**). The wave trains observed throughout summer 1950, resembles an omega-like blocking. Under the influence of this omega-like blocking situation, the storm tracks were shifted northwards and the regions under the influence of the high-pressure system were characterized by warm and dry conditions (**Figures 13A,C**).

Opposite to the 1950 event, the summer 2012 event was more prominent in terms of temperature extremes (**Figures 12B,D**) and to a lesser extent in terms of drought (**Figure 12F**). Summer 2012 was the longest one on record in terms of heat wave duration over large areas in the south-eastern part of Europe, including Croatia, Bosnia and Herzegovina, Serbia, Slovakia, Romania,

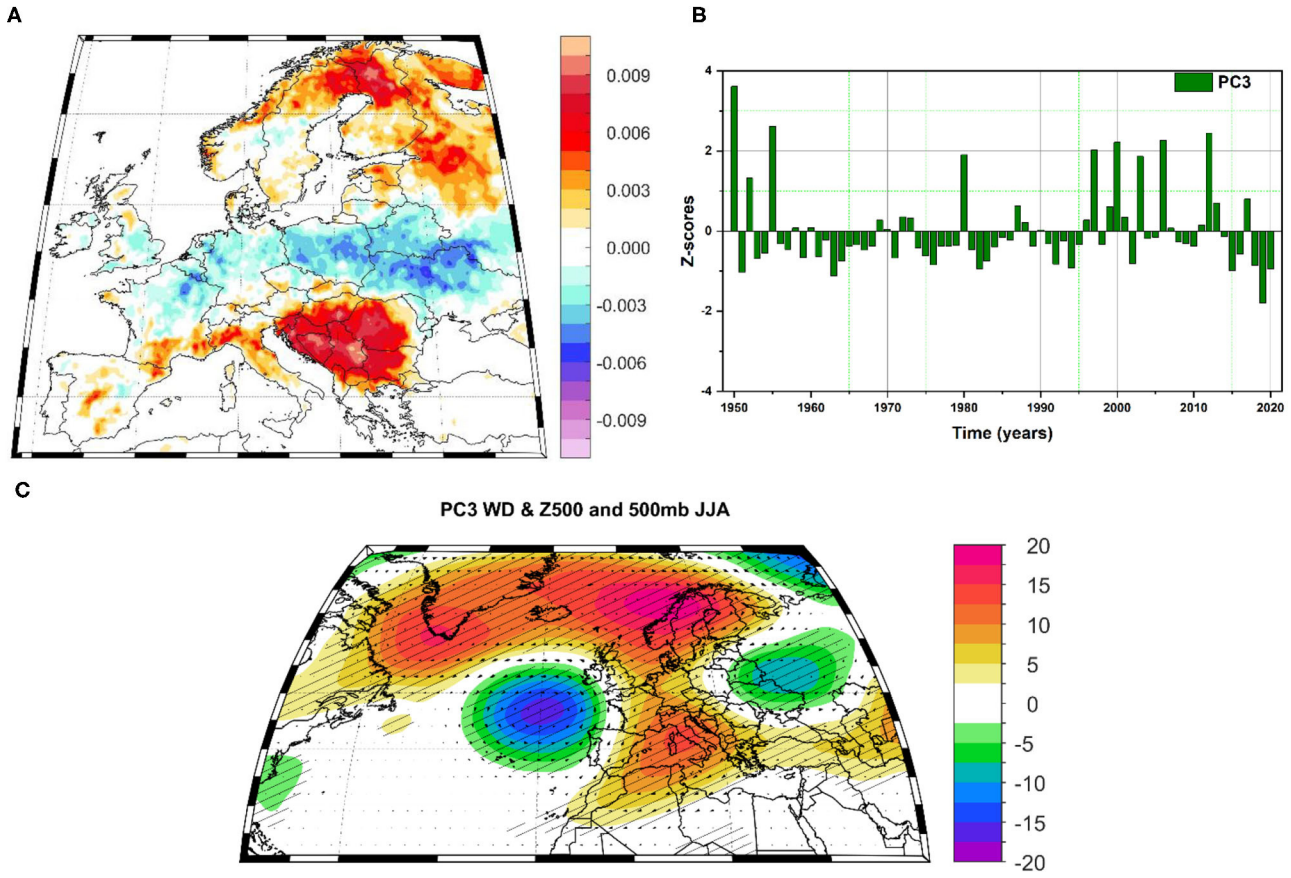

FIGURE 11 | Spatio-temporal variability of compound hot and dry events over the period 1950–2020. **(A)** Third spatial pattern (EOF3); **(B)** the temporal evolution (PC3) corresponding to EOF3; **(C)** The high (PC3 > 1 standard deviation) composite map between PC2 and the summer (JJA) Z500 and the wind vectors at 500 mb. Units: **(C)** Z500 [m].

Ukraine, Moldova, Hungary, and Bulgaria (**Figure 12B**) and the hottest one on record mainly over Romania (**Figure 12D**). Over these regions there were up to 32 days/season with extremely high temperatures (**Figure 13B**). The most affected areas, in terms of drought (**Figures 12D**, **13D**), were Serbia, Bulgaria, and the central part of Romania. The prevailing large-scale circulation, throughout summer 2012 (**Figure 13F**), was characterized by a wave train-like pattern, with positive Z500 anomalies over Greenland, negative Z500 anomalies over the central North Atlantic Ocean, and positive Z500 anomalies extending from the northern part of Africa toward the eastern part of Europe up to Russia. Overall, the spatial distribution of the Z500 anomalies for summer 2012 are different compared to the ones in **Figure 11C**. The highest Z500 anomalies are observed over the region where the hottest and driest conditions were recorded in summer 2012, namely the south-eastern part of Europe (**Figures 13A,D,F**).

CONCLUSIONS

Concurrent hot and dry events (CHDs) can result in significant socio-economic damages, compared to individual events (Leonard et al., 2014). The observed increase in CHDs, which severally impacted the society, economy, and the environment over the past decades, has brought the scientific community to make an extensive analysis of the variability, trends, and future projection of these events, either at global scale (Feng et al., 2020; Ridder et al., 2020; Mukherjee and Mishra, 2021) or at regional scale (Kattsov et al., 2005; Von Buttlar et al., 2018; Hao et al., 2019; Russo et al., 2019; Vogel et al., 2019; Bezak and Mikoš, 2020; Kong et al., 2020). In this respect, we explored the spatio-temporal variability of CHDs at European level and we quantified the relationship between the occurrence of CHDs and the large-scale atmospheric circulation. The study was motivated by the fact, that to our knowledge no study is available at European scale which investigates both the spatio-temporal variability of CHD as well as with their driving factors. This has been accomplished by performing an EOF analysis over the period 1950–2020 on CHDs computed at European scale, in order to analyze the spatio-temporal variability, followed by analyzing the prevailing large-scale atmospheric circulation corresponding to each spatial CHD mode of variability. The main conclusions of this study can be summarized as follows:

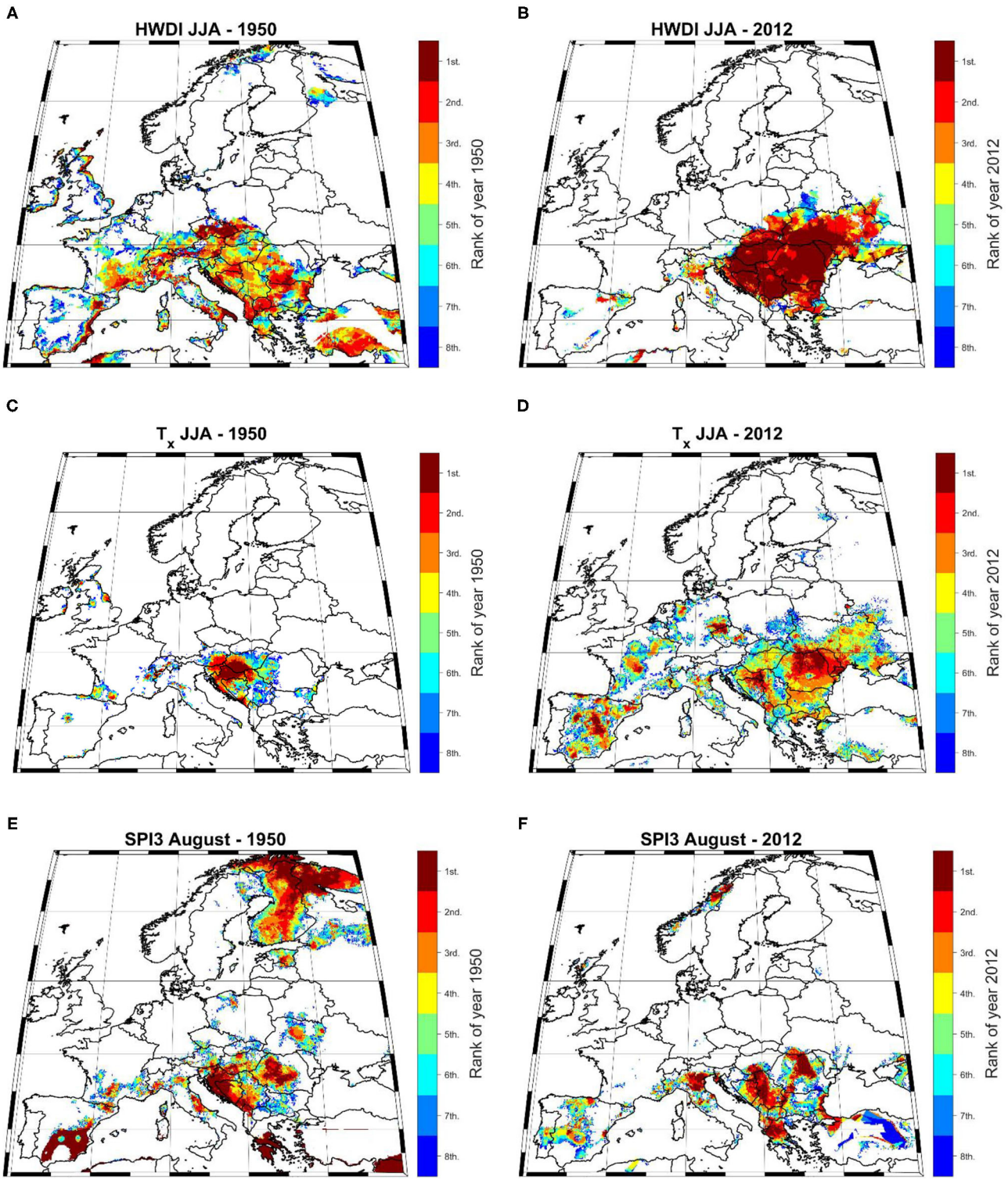

FIGURE 12 | (A) Top-eight ranking of summer 1950 HWDI; **(B)** Top-eight ranking of summer 2012 HWDI; **(C)** Top-eight ranking of summer 1950 T_x; **(D)** Top-eight ranking of summer 2012 T_x; **(E)** Top-eight ranking of 1950 August SPI3; **(F)** Top-eight ranking of 2012 August SPI3. 1st means the longest heatwave (HWDI), hottest (T_x), and driest (SPI3) since 1950, 2nd signifies the second longest, hottest and/or driest, etc., and all ranks >8 are shown in white. Analyzed period: 1950–2020.

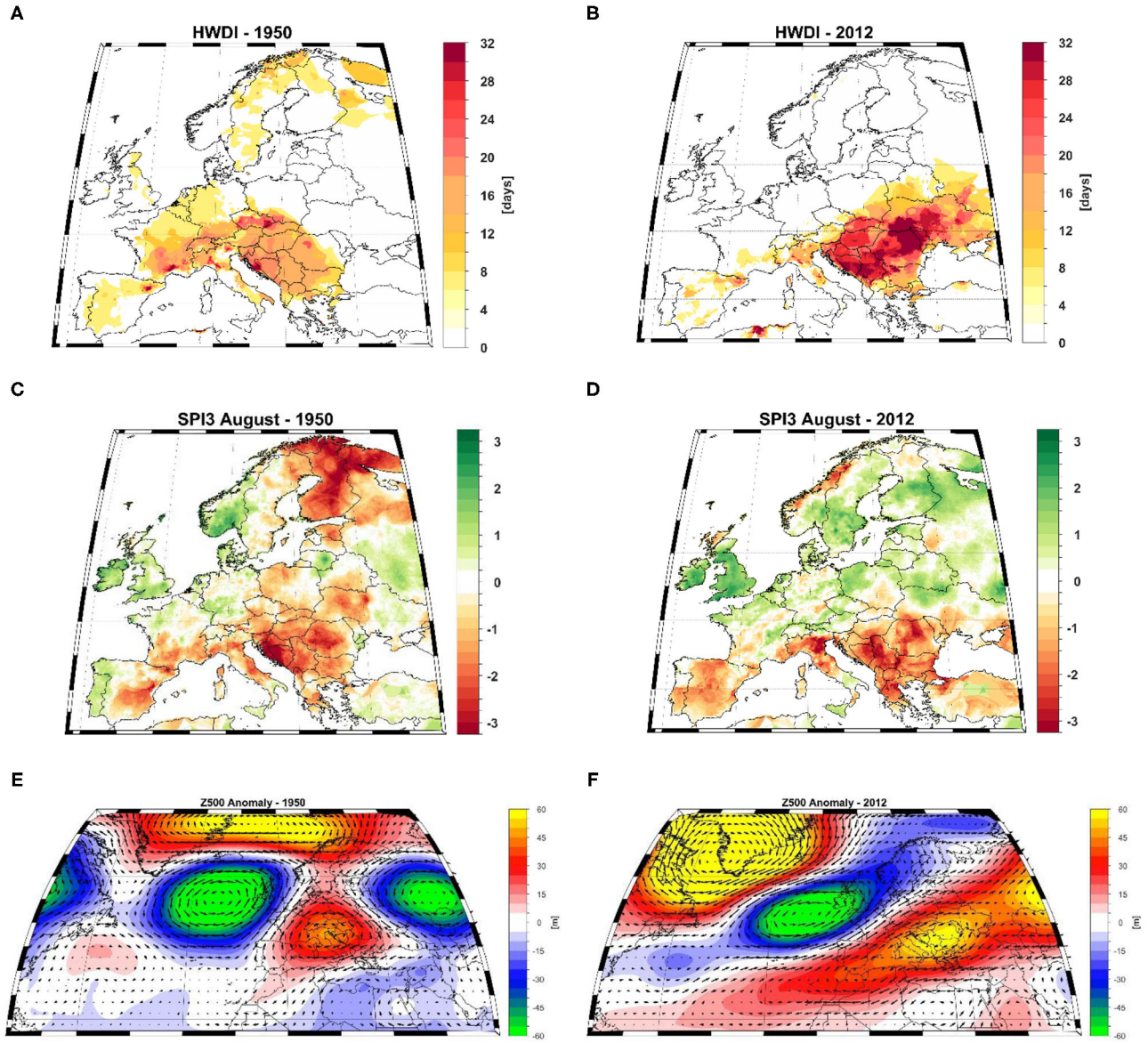

FIGURE 13 | Study cases 1950 and 2012. **(A)** HWDI−1950, **(B)** HWDI−2012; **(C)** August SPI3–1950; **(D)** August SPI3–2012; **(E)** Summer Z500 anomalies−1950 and **(F)** Summer Z500 anomalies−2012. The anomalies are computed relative to the period 1971–2000.

- There is a large variability in the co-occurrence of CHDs at European level over the last ∼70 years. The period 2011–2020 is characterized by an increase in the number of CHD events/decade (∼4 CHD/decade) compared to previous decades, with a special focus on the central and south-eastern part of Europe. The increase in the number of CHD events over the south-eastern part of Europe is mainly due to an increase in the frequency of heatwaves over this region (∼0.20 events/decade), as well as due to an increase in the duration of the heatwaves (∼2 days/decade). In the case of the SPI3, no significant changes at European level have been observed over the last ∼70 years (**Figures 2**, **3**).
- Most of the spatio-temporal variability of CHDs can be explained by the first three EOF patterns which have a preferred center of action. EOF1 has a dipole-like structure, with the highest amplitude over Fennoscandia and the north-western part of Russia, and loadings of opposite sign (but smaller in amplitude) over the Balkans. The years with the most severe CHDs over Fennoscandia, as capture by the temporal evolution of PC1, were: 1955, 1959, 1975, 1997, and 2006, respectively. Summer 1955 stands out as the driest one on record over large regions covering Fennoscandia and the western part of Russia.

- The second mode of variability, represents the spatio-temporal CHDs variability over central Europe, with the highest amplitude over Germany. The years with the most severe CHDs over central Europe, as captured by the temporal evolution of PC2, were: 1976, 2003, 2015, 2018, and 2019, respectively. All these years were characterized by long lasting drought and record breaking temperatures in central Europe (Schär et al., 2004; Rodda and Marh, 2011; Ionita et al., 2017, 2020a; Bakke et al., 2020; Ionita and Nagavciuc, 2020). Summer 2003 ranks as the hottest one on record over northern Spain, France, southern Germany, and large parts of Italy, while summer 2015 ranks as the driest one on record over the eastern part of Austria, the eastern part of Poland, the western part of Ukraine and eastern part of Belarus.
- The third mode of variability is concentrated mainly over the south-eastern part of Europe, with the highest loadings over Romania, Bulgaria, Hungary, Serbia, and Croatia. The driest and warmest summers over the south-eastern part of Europe, based on the temporal evolution of summer PC3, were recorded for the years 1950, 1955, 1980, 1998, 2000, 2003, 2006, and 2012. Summer 2012 ranks as the hottest on record over large areas in the south-eastern part of Europe, where up to 32 days/season with extremely high temperatures were recorded.
- Hot and dry summers are, in general, associated with a persistent high-pressure system over the regions affected by CHDs. CHDs over Fennoscandia are associated with a Z500 pattern resembling the Scandinavian blocking pattern (van der Wiel et al., 2019), characterized by a high-pressure system centered over Fennoscandia, which in turns reduces the zonal flow and diverts the storm tracks southward. CHDs over the central part of Europe, are usually associated with a Rossby wave-train which propagates from the USA to Russia. High frequency of CHDs over the southern part of Europe are associated with a wave train, in the summer Z500 field, characterized by negative Z500 anomalies over central North Atlantic Ocean, positive Z500 anomalies over the south-eastern part of Europe coupled to another center of positive Z500 anomalies over Fennoscandia and negative Z500 anomalies over western Russia.
- Overall, the positive Z500 anomalies associated with each mode of variability largely suppresses ascending motions, reduces water vapor condensation and precipitation formation, leading to drought conditions below this atmospheric system. The high-pressure system acts as a barrier, preventing low-pressure systems from moving over Europe and pushing them instead to the north. The predominance of anticyclonic atmospheric circulation regimes seems to be a prerequisite for the development of very dry and warm summers.

The present study improves our understanding of the spatio-temporal variability of hot and dry summers, at European level, as well as the driving mechanisms of these events. The decadal changes observed over the last ∼70 years in the frequency of CHDs and the fact that over the last decade central Europe seems to become a hot spot of CHDs could potentially help the decision-makes to develop more appropriate mitigation strategies. The results of this study are particularly useful for CHD impact assessment on health risk, energy demands, and agriculture, among others, that are often neglected by the decision-makers and stakeholders.

DATA AVAILABILITY STATEMENT

The original contributions presented in the study are included in the article/**Supplementary Material**, further inquiries can be directed to the corresponding author.

AUTHOR CONTRIBUTIONS

MI designed the study and wrote the paper. DC and VN helped write the paper and interpret the results. All authors contributed to the article and approved the submitted version.

FUNDING

MI was supported by Helmholtz Association through the joint program Changing Earth–Sustaining our Future (PoF IV) program of the AWI. Funding by the AWI Strategy Fund Project–PalEX and by the Helmholtz Climate Initiative–REKLIM is gratefully acknowledged. VN was supported partially by project number PN-III-P1-1.1-PD-2019-0469.

SUPPLEMENTARY MATERIAL

The Supplementary Material for this article can be found online at: https://www.frontiersin.org/articles/10.3389/fclim.2021.688991/full#supplementary-material

REFERENCES

Bakke, S. J., Ionita, M., and Tallaksen, L. M. (2020). The 2018 Northern European hydrological drought and its drivers in a historical perspective. *Hydrol. Earth Syst. Sci.* 24, 5621–5653. doi: 10.5194/hess-24-5621-2020

Barriopedro, D., Fischer, E. M., Luterbacher, J., Trigo, R. M., and García-Herrera, R. (2011). The hot summer of 2010: redrawing the temperature record map of Europe. *Science* 332, 220–224. doi: 10.1126/science.1201224

Barriopedro, D., García-Herrera, R., and Trigo, R. M. (2010). Application of blocking diagnosis methods to general circulation models. Part I: a novel detection scheme. *Clim. Dyn.* 35, 1373–1391. doi: 10.1007/s00382-010-0767-5

Ben-Ari, T., Boé, J., Ciais, P., Lecerf, R., Van Der Velde, M., and Makowski, D. (2018). Causes and implications of the unforeseen 2016 extreme yield loss in the breadbasket of France. *Nat. Commun.* 9:1627. doi: 10.1038/s41467-018-04087-x

Bezak, N., and Mikoš, M. (2020). Changes in the compound drought and extreme heat occurrence in the 1961–2018 period at the European scale. *Water* 12:3543. doi: 10.3390/w12123543

Bueh, C., and Nakamura, H. (2007). Scandinavian pattern and its climatic impact. Q. *J. R. Meteorol. Soc.* 133, 2117–2132. doi: 10.1002/qj.173

Ciais, P., Reichstein, M., Viovy, N., Granier, A., Ogée, J., Allard, V., et al. (2005). Europe-wide reduction in primary productivity caused by the heat and drought in 2003. *Nature* 437, 529–533. doi: 10.1038/nature03972

Cornes, R. C., van der Schrier, G., van den Besselaar, E. J. M., and Jones, P. D. (2018). An ensemble version of the E-OBS temperature and precipitation data sets. *J. Geophys. Res. Atmos.* 123, 9391–9409. doi: 10.1029/2017JD028200

Della-Marta, P. M., Luterbacher, J., von Weissenfluh, H., Xoplaki, E., Brunet, M., and Wanner, H. (2007). Summer heat waves over western Europe 1880-2003, their relationship to large-scale forcings and predictability. *Clim. Dyn.* 29, 251–275. doi: 10.1007/s00382-007-0233-1

Diffenbaugh, N. S., Singh, D., Mankin, J. S., Horton, D. E., Swain, D. L., Touma, D., et al. (2017). Quantifying the influence of global warming on unprecedented extreme climate events. *Proc. Natl. Acad. Sci. U.S.A.* 114, 4881–4886. doi: 10.1073/pnas.1618082114

Feng, S., Wu, X., Hao, Z., Hao, Y., Zhang, X., and Hao, F. (2020). A database for characteristics and variations of global compound dry and hot events. *Weather Clim. Extrem.* 30:100299. doi: 10.1016/j.wace.2020.100299

Fischer, E. M., Seneviratne, S. I., Lüthi, D., and Schär, C. (2007). Contribution of land-atmosphere coupling to recent European summer heat waves. *Geophys. Res. Lett.* 34:L06707. doi: 10.1029/2006GL029068

Geirinhas, J. L., Russo, A., Libonati, R., Sousa, P. M., Miralles, D. G., and Trigo, R. M. (2021). Recent increasing frequency of compound summer drought and heatwaves in Southeast Brazil. *Environ. Res. Lett.* 16:034036. doi: 10.1088/1748-9326/abe0eb

Hao, Z., Hao, F., Xia, Y., Singh, V. P., and Zhang, X. (2019). A monitoring and prediction system for compound dry and hot events. *Environ. Res. Lett.* 14:114034. doi: 10.1088/1748-9326/ab4df5

Hersbach, H., Bell, B., Berrisford, P., Hirahara, S., Horányi, A., Muñoz-Sabater, J., et al. (2020). The ERA5 global reanalysis. *Q. J. R. Meteorol. Soc.* 146, 1999–2049. doi: 10.1002/qj.3803

Hirschi, M., Seneviratne, S. I., Alexandrov, V., Boberg, F., Boroneant, C., Christensen, O. B., et al. (2011). Observational evidence for soil-moisture impact on hot extremes in southeastern Europe. *Nat. Geosci.* 4, 17–21. doi: 10.1038/ngeo1032

Hori, M. E., Inoue, J., Kikuchi, T., Honda, M., and Tachibana, Y. (2011). Recurrence of intraseasonal cold air outbreak during the 2009/2010 winter in Japan and its ties to the atmospheric condition over the Barents-Kara Sea. *Sola* 7, 25–28. doi: 10.2151/sola.2011-007

Ionita, M., Boronean,ʔ, C., and Chelcea, S. (2015). Seasonal modes of dryness and wetness variability over Europe and their connections with large scale atmospheric circulation and global sea surface temperature. *Clim. Dyn.* 45, 2803–2829. doi: 10.1007/s00382-015-2508-2

Ionita, M., Dima, M., Nagavciuc, V., Scholz, P., and Lohmann, G. (2021). Past megadroughts in central Europe were longer, more severe, and less warm than modern droughts. *Commun. Earth Environ.* 2:61. doi: 10.1038/s43247-021-00130-w

Ionita, M., Lohmann, G., Rimbu, N., Chelcea, S., and Dima, M. (2012). Interannual to decadal summer drought variability over Europe and its relationship to global sea surface temperature. *Clim. Dyn.* 38, 363–377. doi: 10.1007/s00382-011-1028-y

Ionita, M., and Nagavciuc, V. (2020). Forecasting low flow conditions months in advance through teleconnection patterns, with a special focus on summer 2018. *Sci. Rep.* 10:13258. doi: 10.1038/s41598-020-70060-8

Ionita, M., and Nagavciuc, V. (2021). Changes in drought features at European level over the last 120 years. *Nat. Hazards Earth Syst. Sci. Discuss.* 2021, 1–31. doi: 10.5194/nhess-2021-46

Ionita, M., Nagavciuc, V., and Guan, B. (2020b). Rivers in the sky, flooding on the ground: the role of atmospheric rivers in inland flooding in central Europe. *Hydrol. Earth Syst. Sci.* 24, 5125–5147. doi: 10.5194/hess-24-5125-2020

Ionita, M., Nagavciuc, V., Kumar, R., and Rakovec, O. (2020a). On the curious case of the recent decade, mid-spring precipitation deficit in central Europe. *Npj Clim. Atmos. Sci.* 3:49. doi: 10.1038/s41612-020-00153-8

Ionita, M., Tallaksen, L. M., Kingston, D. G., Stagge, J. H., Laaha, G., Lanen, H. A. J., et al. (2017). The European 2015 drought from a climatological perspective. *Hydrol. Earth Syst. Sci.* 21, 1397–1419. doi: 10.5194/hess-21-1397-2017

Kattsov, V. M., Källén, E., Cattle, H., Christensen, J., Drange, H., Hanssen-Bauer, I., et al. (2005). "Chapter 4, future climate change: modeling and scenarios for the Arctic," in *Arctic Climate Impact Assessment* (Cambridge: Cambridge University Press), 1042. Available online at: http://www.acia.uaf.edu

Kong, Q., Guerreiro, S. B., Blenkinsop, S., Li, X.-F., and Fowler, H. J. (2020). Increases in summertime concurrent drought and heatwave in Eastern China. *Weather Clim. Extrem.* 28:100242. doi: 10.1016/j.wace.2019.100242

Leonard, M., Westra, S., Phatak, A., Lambert, M., van den Hurk, B., McInnes, K., et al. (2014). A compound event framework for understanding extreme impacts. *WIREs Clim. Change* 5, 113–128. doi: 10.1002/wcc.252

Manning, C., Widmann, M., Bevacqua, E., Van Loon, A. F., Maraun, D., and Vrac, M. (2018). Soil moisture drought in Europe: a compound event of precipitation and potential evapotranspiration on multiple time scales. *J. Hydrometeorol.* 19, 1255–1271. doi: 10.1175/JHM-D-18-0017.1

Manning, C., Widmann, M., Bevacqua, E., Van Loon, A. F., Maraun, D., and Vrac, M. (2019). Increased probability of compound long-duration dry and hot events in Europe during summer (1950–2013). *Environ. Res. Lett.* 14:094006. doi: 10.1088/1748-9326/ab23bf

McKee, T. B., Nolan, J., and Kleist, J. (1993). "The relationship of drought frequency and duration yo time scales," in Eighth *Conference on Applied Climatology 17–22 January 1993* (Anaheim, CA), 1–6.

Mueller, B., and Seneviratne, S. I. (2012). Hot days induced by precipitation deficits at the global scale. *Proc. Natl. Acad. Sci. U.S.A.* 109, 12398–12403. doi: 10.1073/pnas.1204330109

Mukherjee, S., and Mishra, A. K. (2021). Increase in compound drought and heatwaves in a warming world. *Geophys. Res. Lett.* 48:e2020GL090617. doi: 10.1029/2020GL090617

Munich RE (2020). *Heatwaves, Drought, and Forest Fires in Europe: Billions of Dollars in Losses for Agricultural Sector*. Munich: Munich Re.

Najibi, N., Devineni, N., Lu, M., and Perdigão, R. A. P. (2019). Coupled flow accumulation and atmospheric blocking govern flood duration. *Npj Clim. Atmos. Sci.* 2:19. doi: 10.1038/s41612-019-0076-6

North, G. R., Bell, T. L., Cahalan, R. F., and Moeng, F. J. (1982). Sampling errors in the estimation of empirical orthogonal functions. *Mon. Weather Rev.* 110, 699–706.

Perkins, S. E., and Alexander, L. V. (2013). On the measurement of heat waves. *J. Clim.* 26, 4500–4517. doi: 10.1175/JCLI-D-12-00383.1

Raymond, C., Horton, R. M., Zscheischler, J., Martius, O., AghaKouchak, A., Balch, J., et al. (2020). Understanding and managing connected extreme events. *Nat. Clim. Change* 10, 611–621. doi: 10.1038/s41558-020-0790-4

Ridder, N. N., Pitman, A. J., Westra, S., Ukkola, A., Do, H. X., Bador, M., et al. (2020). Global hotspots for the occurrence of compound events. *Nat. Commun.* 11:5956. doi: 10.1038/s41467-020-20502-8

Rimbu, N., Lohmann, G., and Ionita, M. (2014). Interannual to multidecadal Euro-Atlantic blocking variability during winter and its relationship with extreme low temperatures in Europe. *J. Geophys. Res. Atmos.* 119, 13621–13636. doi: 10.1002/2014JD021983

Rodda, J., and Marh, T. (2011). *The 1975-76 Drought–A Contemporary and Retrospective Review*. Bailrigg: Centre for Ecology and Hydrology

Russo, A., Gouveia, C. M., Dutra, E., Soares, P. M. M., and Trigo, R. M. (2019). The synergy between drought and extremely hot summers in the Mediterranean. *Environ. Res. Lett.* 14:014011. doi: 10.1088/1748-9326/aaf09e

Samaniego, L., Thober, S., Kumar, R., Wanders, N., Rakovec, O., Pan, M., et al. (2018). Anthropogenic warming exacerbates European soil moisture droughts. *Nat. Clim. Change* 8, 421–426. doi: 10.1038/s41558-018-0138-5

Schär, C., Vidale, P. L., Lüthi, D., Frei, C., Häberli, C., Liniger, M. A., et al. (2004). The role of increasing temperature variability in European summer heatwaves. *Nature* 427, 332–336. doi: 10.1038/nature02300

Schubert, S. D., Stewart, R. E., Wang, H., Barlow, M., Berbery, E. H., Cai, W., et al. (2016). Global meteorological drought: a synthesis of current understanding with a focus on sst drivers of precipitation deficits. *J. Clim.* 29, 3989–4019. doi: 10.1175/JCLI-D-15-0452.1

Schubert, S. D., Wang, H., Koster, R. D., Suarez, M. J., and Groisman, P. Y. (2014). Northern Eurasian heat waves and droughts. *J. Clim.* 27, 3169–3207. doi: 10.1175/JCLI-D-13-00360.1

Seneviratne, S. I., Nicholls, N., Easterling, D., Goodess, C. M., Kanae, S., Kossin, J., et al. (2012). "Changes in climate extremes and their impacts on the natural physical environment," in *Managing the Risks of Extreme Events and Disasters to Advance Climate Change Adaptation: Special Report of the Intergovernmental Panel on Climate Change*, eds C. B. Field, Q. Dahe, T. F. Stocker, and V. Barros (Cambridge: Cambridge University Press), 109–230.

Trenberth, K. E., and Shea, D. J. (2005). Relationships between precipitation and surface temperature. *Geophys. Res. Lett.* 32:L14703. doi: 10.1029/2005GL022760

van der Wiel, K., Bloomfield, H. C., Lee, R. W., Stoop, L. P., Blackport, R., Screen, J. A., et al. (2019). The influence of weather regimes on European

renewable energy production and demand. *Environ. Res. Lett.* 14:094010. doi: 10.1088/1748-9326/ab38d3

Vicente-Serrano, S. M., Domínguez-Castro, F., Murphy, C., Hannaford, J., Reig, F., Peña-Angulo, D., et al. (2021). Long-term variability and trends in meteorological droughts in Western Europe (1851–2018). *Int. J. Climatol.* 41, E690–E717. doi: 10.1002/joc.6719

Vogel, M. M., Zscheischler, J., Wartenburger, R., Dee, D., and Seneviratne, S. I. (2019). Concurrent 2018 hot extremes across northern hemisphere due to human-induced climate change. *Earth's Futue* 7, 692–703. doi: 10.1029/2019EF001189

Von Buttlar, J., Zscheischler, J., Rammig, A., Sippel, S., Reichstein, M., Knohl, A., et al. (2018). Impacts of droughts and extreme-temperature events on gross primary production and ecosystem respiration: a systematic assessment across ecosystems and climate zones. *Biogeosciences* 15, 1293–1318. doi: 10.5194/bg-15-1293-2018

von Storch, H., and Zwiers, F. W. (1999). *Statistical Analysis in Climate Research*. Cambridge: Cambridge University Press.

Zhang, R. R., Sun, C., Zhu, J., Zhang, R. R., and Li, W. (2020). Increased European heat waves in recent decades in response to shrinking Arctic sea ice and Eurasian snow cover. *Npj Clim. Atmos. Sci.* 3:7. doi: 10.1038/s41612-020-0110-8

Zscheischler, J., Westra, S., van den Hurk, B. J. J. M., Seneviratne, S. I., Ward, P. J., Pitman, A., et al. (2018). Future climate risk from compound events. *Nat. Clim. Change* 8, 469–477. doi: 10.1038/s41558-018-0156-3

Conflict of Interest: The authors declare that the research was conducted in the absence of any commercial or financial relationships that could be construed as a potential conflict of interest.

Table S1. Description of the affected regions and associated impact for six extreme CHDs: 1950, 1959, 2003, 2012 and 2015.

1950	Anomalously dry summer characterized also by high temperatures in central Europe (Briffa et al., 2009); The longest and one of the most severe droughts over European Russia; Rainfall deficit at Pan-European level (Spinoni et al., 2015)
1955	The longest drought event in Fennoscandia; the most affected area was the Northern Europe (Spinoni et al., 2015); Reduced productivity of annual crop cultivation: crop losses, damage to crop quality or crop failure due to dieback, premature ripening, drought-induced pest infestations or diseases, reduced productivity of livestock farming (e.g. reduced yields or quality of milk, reduced stock weights) and increased costs/economic losses in Scandinavia (EDC, 2012)
1959	The most severe drought in Fennoscandia, the most affected area was the northern and eastern part of Europe (Spinoni et al., 2015); Reduced productivity of annual crop cultivation: crop losses, damage to crop quality or crop failure due to dieback, premature ripening, drought-induced pest infestations or diseases, in Northern/Central Europe, reduced productivity of livestock farming in Northern/Central Europe, increased costs/economic losses (458 million euros in Nederland), reduced tree growth and vitality, local water supply shortage / problems (drying up of springs/wells, reservoirs, streams), limitations in water supply to households in rural areas, (temporary) water quality deterioration/problems of surface waters, increased mortality of aquatic species, increased burned area, increased number of wildfires (EDC, 2012)
2003	Severe drought from May to September (EDC, 2013); The most affected areas were central France and eastern Austria (Laaha et al., 2017); Air temperatures were extremely abnormal with monthly anomalies of up to 6 ◦C in a large part of Europe (Rebetez et al., 2006), over 100 million affected people (EU, 2010) and direct economic impacts of 17.134 billion Euro (EEA, 2019); Local limitations and serious shortage problems in public water, decreased the quantity and quality of the harvests, particularly in Central and Southern European agricultural areas; important loss of crops more than 25 000 fires were recorded in Portugal, Spain, Italy, France, Austria, Finland, Denmark and Ireland; the estimation of forest areas destroyed reached 647 069 hectares; decrease in nuclear power production and water use restrictions in 75 % of the French departments; local limitations and serious shortage problems in public water supply (UNEP, 2003);
2012	Severe drought in Romania, grain production fell by almost 40% in Romania, but also in Bulgaria and Hungary (Pana, 2013); Economic costs due to climatological events : 3.909 million Euro (EEA, 2019); In July 2012 there were 16 consecutive days of heat, rainfall deficit, almost the whole month of July with an average temperature of over 32°C; in some regions in Romania, the crop production loss was ~97% (Pavnutescu, 2012); Several localities were left without drinking water due to the prolonged drought, the authorities restricting consumption and transported water by tankers for the population and animals (economica.net, 2012a); Temperatures repeatedly exceeded 35°C in July, from eastern Italy to the Black Sea region and even Ukraine, mean temperature was with about 5 degrees above normal for this period (economica.net, 2012b); In the Republic of Moldova the drought has strained the situation of the cereals market, there has been an increase in market prices of wheat, corn and other cereals, the drought caused a economic crisis (point.md, 2012);
2015	In France, Benelux, western Germany, northern Italy, northern Spain, the Czech Republic, Poland, Ukraine and Belarus the rainfall deficit was greater than 100-130 mm, representing a reduction of about 50-60%, and in some cases even 80%, compared to the long-term average (EDO, 2015); Almost 75% of the area of Germany was under at least moderate drought in July 2015 (Ionita et al., 2017); Maximum daily temperatures consistently above 30°C for durations of 30 to 35 days (DG Environment – European Commission, 2007); The most affected areas were the central and eastern part of Europe and the northern Balkans (Laaha et al., 2017); Restrictions to civil and industrial water uses, losses in agricultural production reductions or even the complete cessation of inland water transportation, increases in forest wildfires, impacts on forestry (e.g. reduced biomass accumulation, insect attacks and diseases), limitations to energy production (hydropower and cooling) (EDO, 2015), Direct economic impacts 2.172 billion Euro (EEA, 2019) and ~1250 related deaths (Munich RE, 2020); Crop losses of up to 50% were reported in the Czech Republic, Germany, Poland and Slovakia, across central Europe and parts of eastern Europe (e.g. Romania) hundreds of towns and villages faced drinking water supply deficiencies (Van Lanen et al., 2016).

References:

Briffa, K. R., van der Schrier, G. and Jones, P. D.: Wet and dry summers in europe since 1750: Evidence of increasing drought, International Journal of Climatology, 29(13), doi:10.1002/joc.1836, 2009.

DG Environment – European Commission: Water Scarcity and Droughts in-depth assessment Second Interim Report – June 2007, The European Commission [online] Available from: https://ec.europa.eu/environment/water/quantity/pdf/comm_droughts/2nd_int_report.pdf, 2007.

economica.net: Seceta începe să lase populaţia din Vaslui fără apă potabilă. ISU intervine în zonele afectate, economica.net [online] Available from: https://www.economica.net/seceta-incepe-sa-lase-populatia-din-vaslui-fara-apa-potabila-isu-intervine-in-zonele-afectate_29975.html, 2012a.

economica.net: Valul de căldură din Europa afectează grav recolta de porumb, în paralel cu seceta din SUA, economica.net [online] Available from: https://www.economica.net/valul-de-caldura-din-europa-afecteaza-grav-recolta-de-porumb-in-paralel-cu-seceta-din-sua_29780.html, 2012b.

EDC: European Drought Impact Inventory Query, European Drought Centre [online] Available from: https://www.geo.uio.no/edc/droughtdb/edr/impactdatabaseresults.php, 2012.

EDC: Drought of 2003, Europe, European Drought Centre [online] Available from: https://www.geo.uio.no/edc/droughtdb/edr/DroughtEvents/_2003_Event.php, 2013.

EDO: Drought News August 2015, EDO Combined Drought Indicator (CDI) –Situation on 31 July 2015. [online] Available from: http://edo.jrc.ec.europa.eu, 2015.

EEA: Economic losses from climate-related extremes in Europe — European Environment Agency, [online] Available from: https://www.eea.europa.eu/data-and-maps/indicators/direct-losses-from-weather-disasters-3, 2019.

EU: Water Scarcity and Drought in the European Union, European Union Publication Office [online] Available from: https://ec.europa.eu/environment/pubs/pdf/factsheets/water_scarcity.pdf, 2010.

Ionita, M., Tallaksen, L. M., Kingston, D. G., Stagge, J. H., Laaha, G., Van Lanen, H. A. J., Scholz, P., Chelcea, S. M., Haslinger, K., Lanen, H. A. J. Van, Chelcea, S. M., Haslinger, K., Scholz, P., Chelcea, S. M. and Haslinger, K.: The European 2015 drought from a climatological perspective, Hydrology and Earth System Sciences, 21, 1397–1419, doi:doi:10.5194/hess-21-1397-2017, 2017.

Laaha, G., Gauster, T., Tallaksen, L. M., Vidal, J. P., Stahl, K., Prudhomme, C., Heudorfer, B., Vlnas, R., Ionita, M., Scholz, P., Van Lanen, H. A. J., Adler, M. J., Caillouet, L., Delus, C., Fendekova, M., Gailliez, S., Hannaford, J., Kingston, D., Van Loon, A. F., Mediero, L., Osuch, M., Romanowicz, R. J., Sauquet, E., Stagge, J. H. and Wong, W. K.: The European 2015 drought from a hydrological perspective, Hydrology and Earth System Sciences, 21(3), 3001–3024, doi:10.5194/hess-21-1397-2017, 2017.

Van Lanen, H. A. J., Laaha, G., Kingston, D. G., Gauster, T., Ionita, M., Vidal, J. P., Vlnas, R., Tallaksen, L. M., Stahl, K., Hannaford, J., Delus, C., Fendekova, M., Mediero, L., Prudhomme, C., Rets, E., Romanowicz, R. J., Gailliez, S., Wong, W. K., Adler, M. J., Blauhut, V., Caillouet, L., Chelcea, S., Frolova, N., Gudmundsson, L., Hanel, M., Haslinger, K., Kireeva, M., Osuch, M., Sauquet, E., Stagge, J. H. and Van Loon, A. F.: Hydrology needed to manage droughts: the 2015 European case, Hydrological Processes, 30(17), 3097–3104, doi:10.1002/hyp.10838, 2016.

Munich RE: Heatwaves, drought and forest fires in Europe: Billions of dollars in losses for agricultural

sector. [online] Available from: https://www.munichre.com/topics-online/en/climate-change-and-natural-disasters/climate-change/heatwaves-and-drought-in-europe.html, 2020.

Pana, M.: Agricultura – scădere drastică în 2012: Seceta nu justifică prăbușirea randamentelor, cursdeguvernare.ro [online] Available from: https://cursdeguvernare.ro/agricultura-scadere-drastica-in-2012-seceta-nu-justifica-prabusirea-randamentelor.html, 2013.

Pavnutescu, M.: Cea mai mare seceta, din ultimii 50 de ani, green-report.ro [online] Available from: https://www.green-report.ro/cea-mai-mare-seceta-din-ultimii-50-de-ani/, 2012.

point.md: Seceta din 2012 provoacă o nouă criză economică, pointnews.md [online] Available from: https://point.md/ru/novosti/ekonomika/seceta-din-2012-provoaca-o-noua-criza-economica, 2012.

Rebetez, M., Mayer, H., Dupont, O., Schindler, D., Gartner, K., Kropp, J. P. and Menzel, A.: Heat and drought 2003 in Europe: a climate synthesis, Annals of Forest Science, 63(6), 569–577, doi:10.1051/forest:2006043, 2006.

Spinoni, J., Naumann, G., Vogt, J. V. and Barbosa, P.: The biggest drought events in Europe from 1950 to 2012, Journal of Hydrology: Regional Studies, 3, 509–524, doi:10.1016/j.ejrh.2015.01.001, 2015.

UNEP: Impacts of summer 2003 heat wave in Europe, Environment Alert Bulletin, 2, 1–4, 2003.